

Article

Influence of Recycled Plastic Incorporation as Coarse Aggregates on Concrete Properties

Khawar Ali ¹, Panumas Saingam ², Muhammad Irshad Qureshi ^{1,3}, Shahzad Saleem ¹, Adnan Nawaz ⁴, Tahir Mehmood ⁴, Ahsen Maqsoom ⁴, Muhammad Waqas Malik ⁵ and Suniti Suparp ^{6,*}

- ¹ Department of Civil Engineering, University of Engineering and Technology, Taxila 47050, Pakistan
² Department of Civil Engineering, School of Engineering, King Mongkut's Institute of Technology Ladkrabang, Bangkok 10520, Thailand
³ Department of Civil and Environmental Engineering, Washington State University, Pullman, WA 99164, USA
⁴ Department of Civil Engineering, COMSATS University Islamabad, Wah Campus, Wah Cantt 47040, Pakistan
⁵ Department of Civil Engineering, Capital University of Science & Technology, Islamabad 44000, Pakistan
⁶ Department of Civil and Environmental Engineering, Faculty of Engineering, Srinakharinwirot University, Nakhonnayok 26120, Thailand
* Correspondence: suniti@g.swu.ac.th

Abstract: Plastic waste has increased significantly in recent years as a result of fast population growth and urbanization. Studies on the incorporation of plastic aggregates as a substitution for natural aggregates in concrete are needed to successfully reduce both adverse environmental impact and the depletion of natural resources. The objective of this research was to investigate the use of plastic as a partial substitution for natural coarse aggregates in concrete. For this purpose, seven concrete mixes were produced using 0, 10, 15, and 20% plastic coarse aggregates to replace natural aggregates with and without silica fume of similar replacement levels with cement. Fresh density, workability, compressive strength, splitting tensile strength, stress–strain response, and Poisson's ratio were observed to study the fresh as well as hardened properties of concrete mixtures. Indoor and outdoor thermal performance and thermo-gravimetric analysis were also investigated. The results revealed that the plastic aggregates' incorporation improved the workability of concrete; however, it negatively influenced the fresh density and mechanical properties of concrete. The compressive and tensile strengths of plastic aggregate concrete without silica fume were reduced by 32 and 33%, respectively. The reduction in strength could be associated with the smooth texture of plastic aggregates. The addition of silica fume with plastic aggregates resulted in denser concrete and improved mechanical properties. In general, the performance of plastic aggregates as a partial replacement for natural aggregates was satisfactory, which suggests their possible use to produce eco-friendlier concrete.

Keywords: plastic waste; sustainability; silica fume; stress–strain behavior; thermal performance; recycling



Citation: Ali, K.; Saingam, P.; Qureshi, M.I.; Saleem, S.; Nawaz, A.; Mehmood, T.; Maqsoom, A.; Malik, M.W.; Suparp, S. Influence of Recycled Plastic Incorporation as Coarse Aggregates on Concrete Properties. *Sustainability* **2023**, *15*, 5937. <https://doi.org/10.3390/su15075937>

Academic Editors: Liborio Cavaleri and Miguel Bravo

Received: 29 December 2022

Revised: 21 February 2023

Accepted: 21 March 2023

Published: 29 March 2023



Copyright: © 2023 by the authors. Licensee MDPI, Basel, Switzerland. This article is an open access article distributed under the terms and conditions of the Creative Commons Attribution (CC BY) license (<https://creativecommons.org/licenses/by/4.0/>).

1. Introduction

Concrete, a combination of cement, coarse aggregates, sand, water, and other inert materials, is the most commonly used construction material in the world. Worldwide, per capita concrete consumption is estimated to be approximately 3 times as much as it was 4 decades ago with around 30 billion tons of concrete produced annually, and the number is expected to rise [1]. The aggregates typically account for 65–80% of the total volume of concrete and have a significant impact on the fresh and hardened properties of the cementitious matrix [2]. Due to the massive concrete production around the globe, natural resources are rapidly depleting, resulting in stringent environmental impacts [3]. The worldwide aggregate production market forecasts a 59% increase in aggregate consumption by the end of 2025 [4]. The mining of sand and gravel is one of the major challenges to sustainability in the twenty-first century [5] because, as compared to other mined and

traded commodities, these minerals are among the least controlled in many regions. The preservation of natural raw materials is essential to curtail the damaging effects of climate change and to avoid natural resource exhaustion in the future. Hence, the possibility of incorporating different alternatives of natural aggregates in concrete has been explored by several researchers [6–9], mostly employing construction and demolition waste as recycled aggregates [10] as well as solid waste, such as glass [11], cardboard, paper [12], bricks [13], crumb waste tires [14], etc.

Plastic, a versatile, resilient, and durable material, is extensively utilized in a wide range of applications, with a global output estimation of 359 million tons in 2018 [15], out of which only 8.8% and 31% were reused in the United States and Europe, respectively. Plastic pollution is a big environmental and ecological concern because it affects agricultural productivity, lowers the potential of the groundwater to recharge, and is a major source of water pollution, all of which have detrimental consequences for marine life [16]. A study conducted by the United Nations Environmental Program in 2006 discovered 46,000 pieces of plastic floating in a square mile of the ocean [17,18], termed the Garbage Patch, that accounts for 90% of all floating garbage in the ocean [1]. Several studies have been undertaken to enhance the recycling of plastic products by integrating plastic into various industrial products. The concrete industry has also adopted the aforementioned solution to partially replace natural aggregates in concrete with plastic waste aggregates [16,19–25] not only to avoid the environmental pollution caused by plastic but also to reduce dependency on the natural sources of concrete raw materials to conserve the environment.

Researchers have analyzed the plastic aggregate (PA) as a substitution for natural aggregates in the form of shredded bottles, pallet shapes, fine pallets, coarse flakes, and fine flakes derived from various industrial products [26]. The literature suggests that incorporating plastic aggregates as a partial replacement for natural aggregates imparts a significant effect on most concrete properties. It has been reported that workability, concrete density, and mechanical parameters, such as compressive strength (CS), splitting tensile strength (STS), and modulus of elasticity (E), decrease dramatically with increased plastic content in concrete mixtures containing shredded plastic particles [25,27–31]. Increasing the percentage of plastic in cement mortar and concrete from 20 to 100% reduced the mixture density up to 50% [24,32–36]. Additionally, it has been discovered that replacing 20–100% of natural sand with plastic aggregates reduced the 28-day compressive strength of concrete by 70% [23,24,27,28,35,37]. Choi et al. [37,38] stated that polyethylene terephthalate (PET) lightweight concrete exhibited a 46% higher slump than that of natural concrete. However, a reduction in workability (7 to 28%) was noticed when lightweight coarse aggregates were entirely substituted with manufactured aggregates [39–42]. Rabar et al. [21] extensively reported the impact of several types of recycled plastic aggregates (RPAs) on the fresh and mechanical characteristics of concrete and indicated that the incorporation of RPAs reduces the mechanical characteristics of concrete. Joseph et al. [43] incorporated shredded PET plastic bottles as a partial replacement for aggregates at a rate of 1.5–4.5% by total volume during concrete batching. The concrete properties were degraded though the inclusion of PET aggregates, causing a reduction of w/c from 0.55 to 0.46, effectively reducing the porosity and restoring concrete performance. Furthermore, the impact resistance, energy absorption, and residual CS of concrete incorporating plastic waste as aggregates were examined by Saxena et al. [44], and it was stated that the CS was reduced due to a poor cohesive bond between the cement paste and the plastic aggregates, but impact strength was enhanced due to the ductile nature of plastic.

In recent years, the use of electronic waste (E-waste) in concrete has caught the attention of researchers, as it is a relatively new phenomenon compared to the use of other forms of plastic in concrete. The recycling of E-waste as a partial substitution of aggregates in concrete can result in reducing the harmful effects of plastic pollution on the environment. Recycling E-waste can have several advantages [45], such as a reduction in solid waste and hence energy consumption; a reduction in landfill cost; a reduction in fuel cost and self-weight of structure [46], as it is lightweight compared to natural aggregates;

and a comparatively lower production cost. However, the research indicates that E-waste aggregates affect the strength mechanical characteristics of concrete, restricting its use.

Prasanna et al. [47] incorporated broken E-waste in concrete as a replacement for natural aggregates and concluded that the E-waste aggregate content should not be more than 20% of the natural aggregates, as it can lead to a reduced CS by 33%. It was also observed that the integration of fly ash in the concrete mixture can help in partially recovering CS. Nadhim et al. [16] also concluded with similar results while incorporating smashed E-waste aggregates along with fly ash in concrete mixtures. Another study [48] examined the effect of shredded E-waste aggregates on the strength properties of concrete and reported that although 15% E-waste can lead to around a 35% reduction in CS, the simultaneous incorporation of 10% fly ash in the concrete mix results in almost equivalent mechanical properties compared to the control mix. Alagusankareswari et al. [49] employed ground E-waste as a partial replacement for coarse aggregates and noticed a considerable weight reduction in the resulting concrete along with lower CS and STS values compared to the control mix for 10%, 20%, and 30% E-waste aggregates.

A brief review of the current literature reveals that the research associated with E-waste concrete has mainly employed non-manufactured plastic aggregates involving sorting, washing, shredding, or crushing plastic waste. Nevertheless, there is a lack of exploration of modifying E-waste with an appropriate heating process [45,50] and producing plastic coarse aggregates with shapes and sizes comparable to natural aggregates. Furthermore, although several studies have examined the fresh and mechanical properties of E-waste-incorporated concrete mixtures, there is a lack of research on investigating the thermal properties of E-waste concrete, i.e., indoor and outdoor thermal performance and thermogravimetric analysis. In the current study, manufactured E-waste aggregates of comparable shape and size to natural coarse aggregates were incorporated in concrete mixtures as a partial replacement for coarse aggregates to examine the fresh and mechanical properties, stress–strain behavior, and thermal performance of concrete containing E-waste aggregates. Moreover, an analytical study was carried out to compare the experimental results of compressive and splitting tensile strengths with those predicted by various codes and past studies.

2. Materials and Methods

2.1. Materials and Mix Proportions

Ordinary Portland cement (Type I) satisfying the requirements of ASTM C150 was used in this research. Silica fume (SF) was used in the concrete mix to enhance the mechanical properties of concrete with PA. Lawrencepur sand with a size below 4.75 mm was used as fine aggregate, while the coarse aggregates of size 4.75 to 19 mm were obtained from the Margalla quarry. For plastic aggregate production, E-waste was used as the primary source. Usually, E-waste needs to be processed through four stages to produce aggregates, as described by a previous study of the same research group [51]. Figure 1 depicts an experimental setup of aggregate production. At the start, the E-waste was washed with water to remove any dust and clay particles. The E-waste was then crushed in an electronic crusher until it was reduced to smaller shredded particles. In the third stage, E-waste material was heated at 200 °C in a kiln. Plastic flakes were melted and then cooled in water to form plastic rocks, which were then crushed to produce plastic aggregates in the last step. The type of plastic used to produce PA was acrylonitrile butadiene styrene (ABS) consisting of laptop scrap, LCDs, monitors, and printers. Figure 2 shows the materials used in this study.

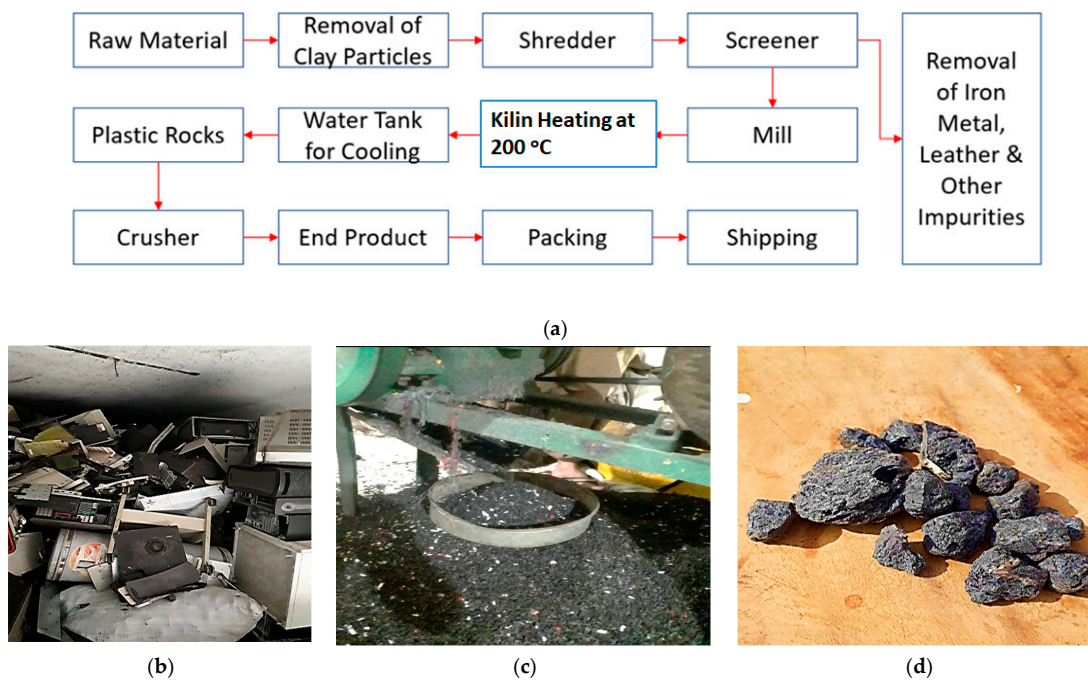


Figure 1. (a) Steps involved in the production of plastic aggregates [51], (b) scrap E-waste, (c) shredded E-waste after crushing, (d) plastic aggregate [6].

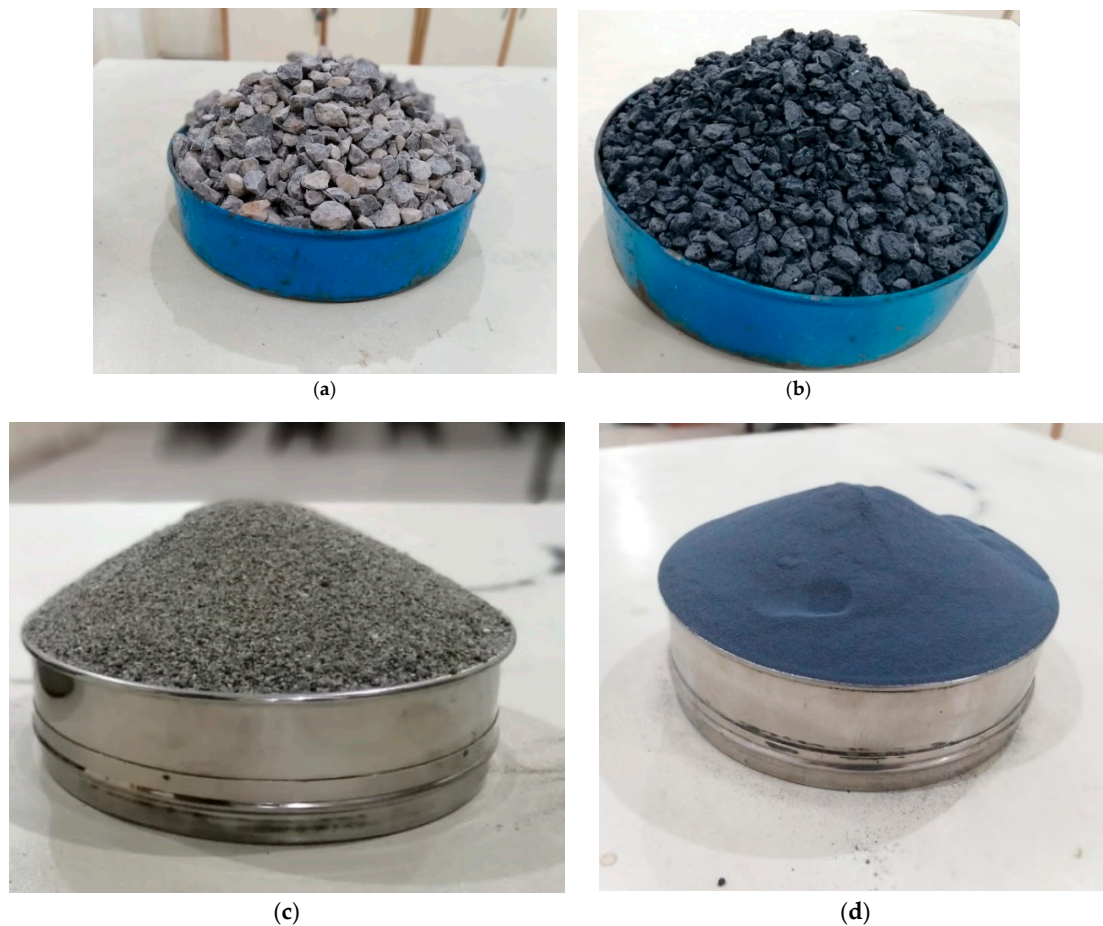


Figure 2. Materials used: (a) natural coarse aggregates; (b) plastic aggregates; (c) natural sand; (d) silica fume.

The physical properties of natural and plastic aggregates are given in Table 1. Specific gravity and water absorption of aggregates were calculated following ASTM C127 [52], and the density test was performed according to ASTM C330 [53]. Sieve analysis was performed as per ASTM C136 [54] to determine the gradation of aggregates. As shown in Table 1, the water absorption and density of PA were found to be 0% and 620 kg/m³ compared to 0.8% and 1518 kg/m³ for natural aggregates, respectively. Results indicate that plastic aggregates were non-absorbent of water and 49.3% lighter in weight than natural aggregates. An optical microscope observed the shape and texture of natural and plastic coarse aggregates. The plastic aggregates seemed to be more porous and angular than the natural ones. The morphology of coarse and plastic aggregates was similar, as discussed later in Section 3.9.

Table 1. Material specifications.

Properties	Nominal Size	Water Absorption (%)	Specific Gravity	Bulk Density (kg/m ³)	Abrasion Value (%)	Impact Value (%)
Cement	50 um	-	3.15	1440	-	-
Sand	-	4	2.67	1600	-	-
Coarse aggregate	20 mm	0.8	2.62	1518	13	10.9
Plastic aggregate	20 mm	0	0.97	620	8.68	2.24
Silica fume	150 nm	-	2.22	784	-	-
Plasticizer	-	-	1.15	-	-	-

In this study, seven mixes were considered with a mix ratio of 1:1.5:3 and a water-binder ratio of 0.45, as shown in Table 2. The first mix represents the control mix. In the second, third, and fourth mixes, natural coarse aggregates were replaced by volumes of 10, 15, and 20% of PA without adding SF. Furthermore, SF was also added along with PA in the remaining mixes by the volume replacement of 10, 15, and 20% of cement. A plasticizer weighing 1.5% of the binder content was incorporated to improve the quality of fresh concrete. The sample mixes were named as given in Table 2. For instance, the mix with 10% PA was termed M10PA, and the mix incorporating SF was named M10PAS.

Table 2. Mix design of concrete mixes.

Specimen ID	Control	M10PA	M15PA	M20PA	M10PAS	M15PAS	M20PAS
Cement (kg/m ³)	392	392	392	392	353	333	314
Silica fume (kg/m ³)	0	0	0	0	21.95	32.93	43.9
Sand (kg/m ³)	661	661	661	661	661	661	661
Coarse aggregate (kg/m ³)	1256	1130.4	1067.6	1004.8	1130.4	1067.6	1004.8
Plastic aggregate (kg/m ³)	0	26.04	39.06	52.08	26.04	39.06	52.08
Water (kg/m ³)	176	176	176	176	169	165	161
Plasticizer (kg/m ³)	4.9	4.9	4.9	4.9	4.7	4.6	4.5

2.2. Testing Details

The fresh properties of concrete, including slump and fresh density, along with dry density, CS, STS, stress–strain behavior, and lateral–longitudinal strains, were determined for hardened concrete. In addition, the morphology of the natural and plastic aggregates and the microstructure were also studied using an optical microscope and scanning electron microscope (SEM). Properties of concrete mixtures were obtained at 28 days of age according to the standard procedures mentioned in the following paragraph. Indoor and outdoor thermal performance was also observed, as discussed in Section 4.

The details of the experiment and standards ASTM C143/C143M [55] and ASTM C138/C138M [56] were used for workability and fresh density measures. Similarly, BS EN 12390-7 [57] and BS EN 12390-6 [58] were used for dry density and splitting tensile strength

measures, respectively. ASTM standards were used for compressive strength and modulus of elasticity measurements. (ASTM C39/C39M [59], ASTM C469 [60]).

2.3. Specimen Preparation

In this study, cylinders of size 100 × 200 mm (Diameter × Height) were cast following the BS EN 12390-6 [58] standards for splitting strength, whereas cylinders of size 150 × 300 mm (Diameter × Height) were cast following the ASTM C39/C39M [59] standards for compression tests. Steel molds were used for both types of cylinders, i.e., splitting and compression tests. The concrete was mixed thoroughly and placed in the steel molds. A proper vibration method was used to compact the concrete.

3. Results and Discussion

3.1. Workability

Workability assures that concrete can be easily handled and has an impact on its structural applications. The effect of plastic aggregates on the workability of fresh concrete was examined using the slump test, and the results are shown in Figure 3. The slump of PA concrete mixtures ranged from 121 mm for the 10% PA mix to 155 mm for the 20% PA mix compared to the much lower slump of 23 mm for the control mix. The higher slump values in the case of PA concrete can be due to the hydrophobic nature, lower water absorption capacity, and relatively smoother texture of PA compared to the natural aggregates. Other researchers have also reported a similar observation [61–63]. This could be beneficial during casting and pumping concrete over long distances and in congested reinforcement areas.

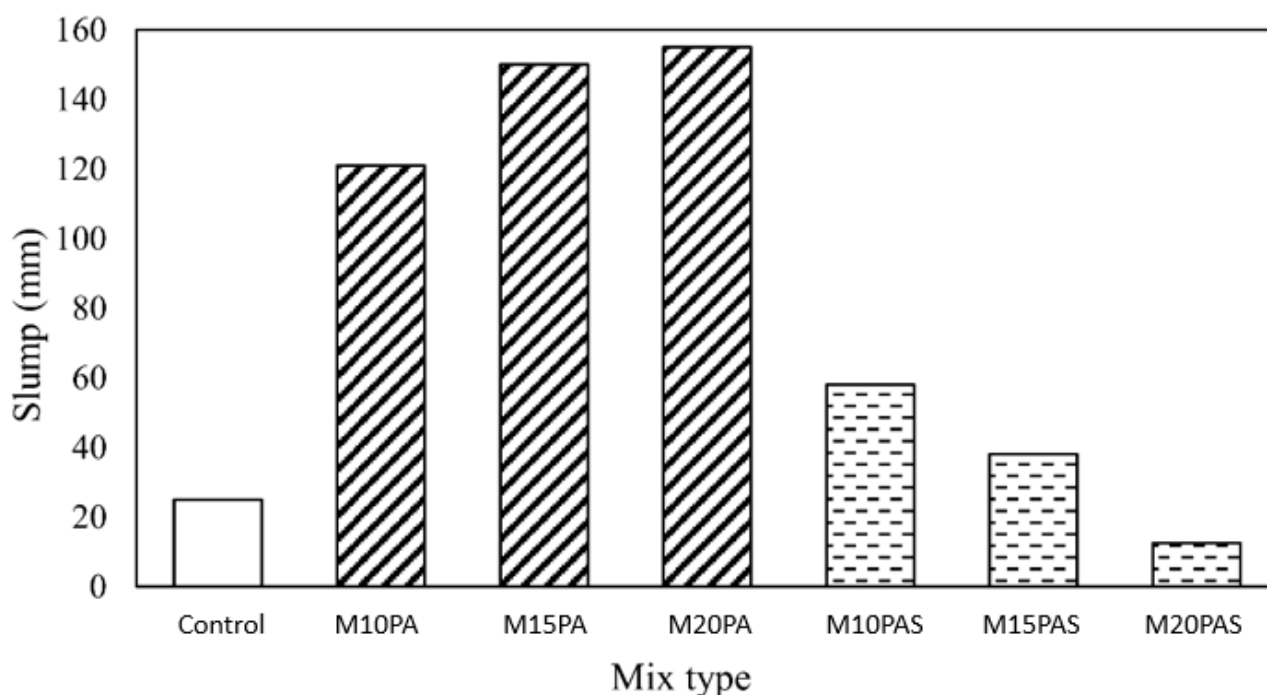


Figure 3. The slump results of various mixtures.

In contrast, the slump of PA concrete mixtures was reduced significantly due to the addition of SF, as demonstrated in Figure 3, where the slump decreased from 58 to 12.5 mm when the percentage of SF increased from 10 to 20%, respectively. This reduction could be attributed to a very fine particle size and the large surface area of SF. The homogeneity of the concrete mix was verified by cutting the PA concrete samples after 28 days. It can be observed from Figure 4 that the resulting concrete was homogeneous, and no segregation was detected.

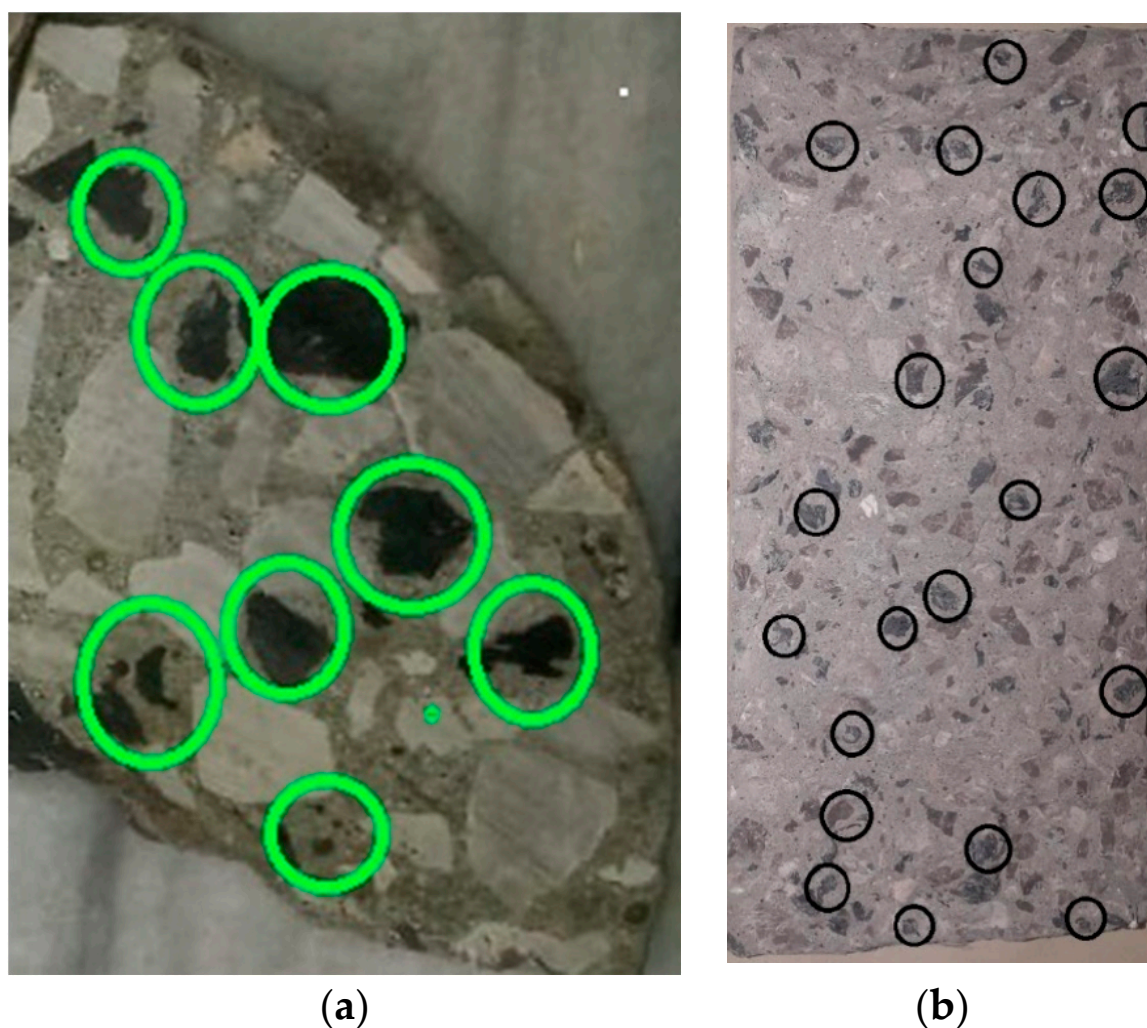


Figure 4. Plastic coarse aggregate concrete specimen: (a) cross-sectional view; (b) longitudinal section view.

3.2. Fresh and Dry Density

The fresh and dry densities of all mixes are illustrated in Figure 5. It can be noticed that the density of concrete declined with an increase in the PA content for both mixture types, i.e., with and without SF. The maximum reduction was observed for a 20% addition of PA with and without SF. This reduction in density could be attributed to the lower densities of plastic aggregates and silica fume, i.e., 760 kg/m^3 and 784 kg/m^3 , respectively, compared to 1518 kg/m^3 and 1440 kg/m^3 of natural aggregates and cement, respectively. Concrete comprises 50–60% of coarse aggregates, so the significant contribution to the density reduction could be attributed to the coarse aggregate replacement. On the other hand, the contribution of SF to a lower density was not very significant due to its lower substitution rate than the PA. This result is also in line with prior studies, which found that replacing conventional aggregates with PA reduced fresh and dry density [16,24,25,31,64–66]. There is a consensus in the literature that incorporating either fine or coarse plastic aggregates reduces the dry density of concrete mixes. This suggests that the replacement percentage of the plastic aggregates can be increased for producing lightweight concrete. Lightweight concrete can help reduce the size of structural members, ultimately lowering the overall cost of the material, handling, and transportation.

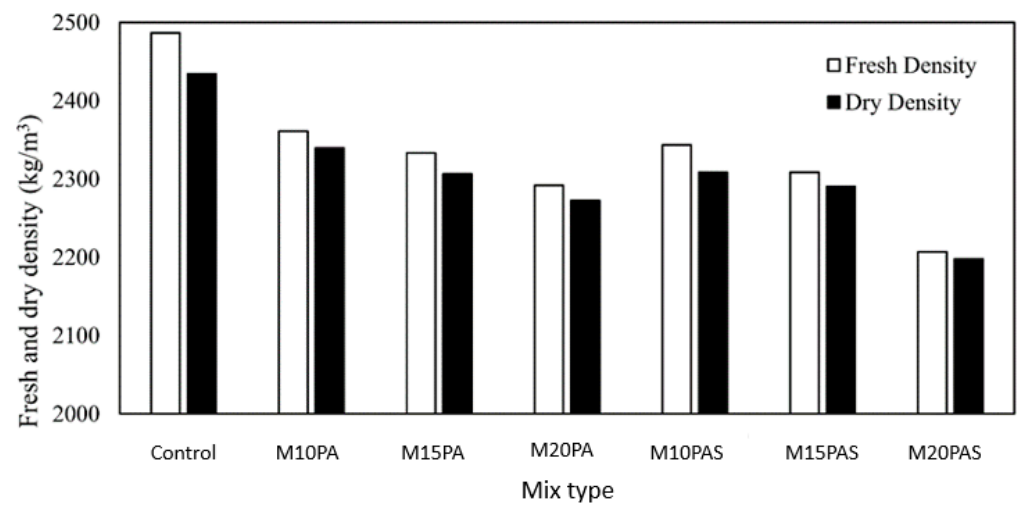


Figure 5. Density results in both fresh and dry conditions.

3.3. Compressive Strength

The CS results of the concrete mixes examined in this research are illustrated in Figure 6. The control mix exhibited a CS of 42.1 MPa. It is to be noted that the CS decreased with an increase in the replacement percentage of PA, as also noticed in previous research [33,67–70]. It can be observed that for 10, 15, and 20% replacement levels, the CS decreased by 31.5, 37.5, and 42.3% for mixtures without SF and by 25.6, 28.6, and 31.5% for blends with SF, respectively. It is interesting to note that the addition of SF partially recovered the loss of CS due to the addition of PA. For example, in the case of 20% replacement, the strength was improved from 24.5 to 29 MPa with SF. This strength gain could be attributed to the pozzolanic activity and finer particle size of SF compared to cement. Previous research agrees that CS increases with an increase in the substitution level of SF [2,29,30,47,60,67–71]. The reduction in CS pertained to the weak interfacial transition zone between the cement paste and plastic aggregates [24,72–77]. As a result, the PA and cement matrix bond was weaker. Another reason for the reduction in PA concrete CS was the higher amount of bleeding water than conventional concrete mixes because PAs are hydrophobic and non-absorbent in nature [39]. The water located near the PA tends to produce a weak bond between the plastic and cement matrix, and the smooth surface of the plastic aggregate also facilitated it.

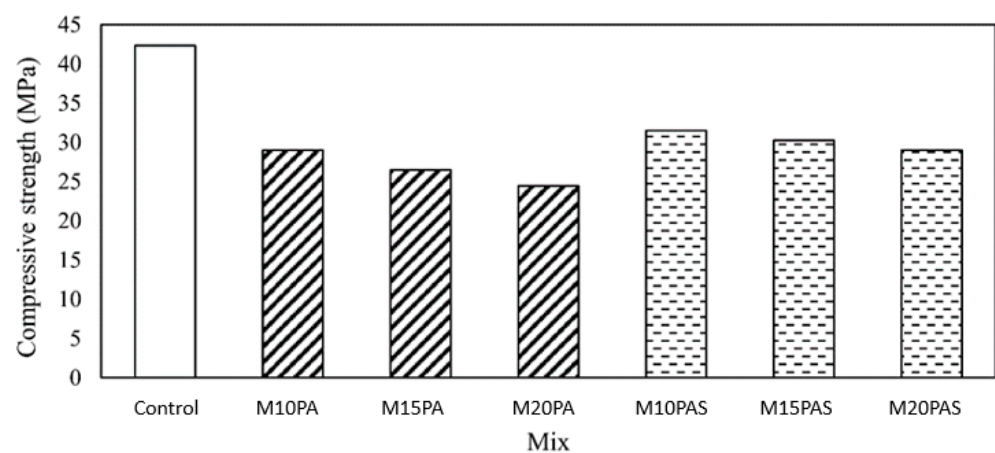


Figure 6. Compressive strength results for various mixes.

3.4. Splitting Tensile Strength

The STS results of concrete blends are shown in Figure 7. The control mix exhibited an STS of 4.5 MPa. Similar to the CS, a reduction in STS was observed with increased PA

content. Figure 7 shows that for 10, 15, and 20% replacement levels, the STS decreased by 32.0, 33.1, and 37.0% for mixtures without SF and 24.1, 25.6, and 32.3% for blends with SF, respectively. The loss of STS due to the addition of PA was also partially recovered by the silica fume incorporation. For example, in the case of 20% replacement, the STS improved from 2.86 to 3.05 MPa with the SF incorporation. The loss of STS due to the replacement of PA has also been reported by various previous studies [38,71,78]. The reason for the decline in STS was similar to that for CS, which mainly includes a weaker ITZ of the concrete. It was also due to the hydrophobic nature, smooth surface, relatively spherical shape, and zero water absorption of plastic aggregates.

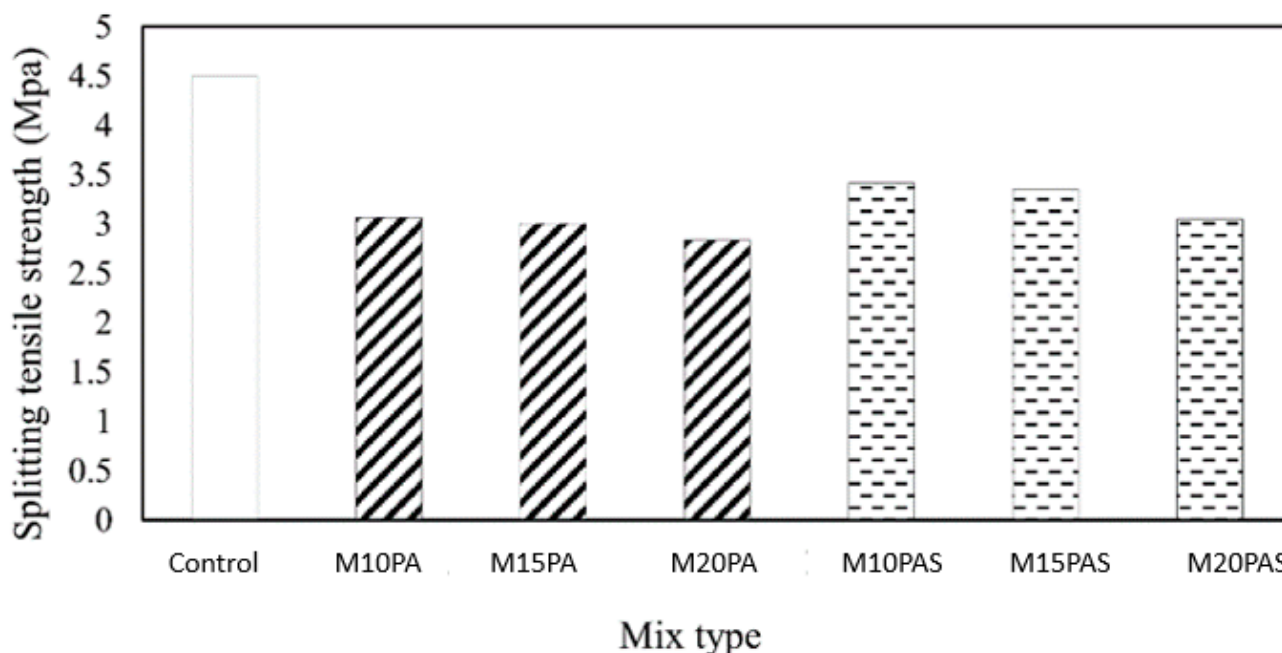


Figure 7. Splitting tensile strength of various mixes.

3.5. Modulus of Elasticity

The modulus of elasticity, or E-value, is affected by the composition of the blend, the quality of aggregate, and the quality of the interfacial transition zone. The modulus of elasticity results are shown in Figure 8 for the specimens of this study. The E-value of concrete mixes relates to the 40% CS of the stress–strain graph, commonly known as the secant slope method. Compared to the E-value of the reference mix (22.2 GPa), it decreased with an increase in the PA replacement percentage for both types of mixtures, i.e., with and without SF. Figure 8 shows that for 10, 15, and 20% replacement levels, the E-value decreased by 4.0, 11.7, and 20.3% for mixtures without SF and by 7.2, 25.6, and 34.2% for blends with SF, respectively. Interestingly, SF addition further reduced the E-value, particularly at a higher substitution level. Previous studies also confirm that the stiffness and E-values of concrete mixtures are inversely proportional to their PA content. Liu et al. [79] substituted virgin sand with pieces of plastic and found that E-value decreased as the replacement level increased. The E-value was determined to be 20.3% lower when 20% of the PA was replaced, which was higher than the highest drop observed in the current study with fabricated PA. The cement matrix and PA exhibited a weaker bond between them, which led to the overall decrease in E-values. Furthermore, the stiffness of concrete constituents demonstrated a significant impact on the modulus of elasticity, as an increasing proportion of PA substituted stiffer natural aggregates, resulting in lower elastic modulus values [16].

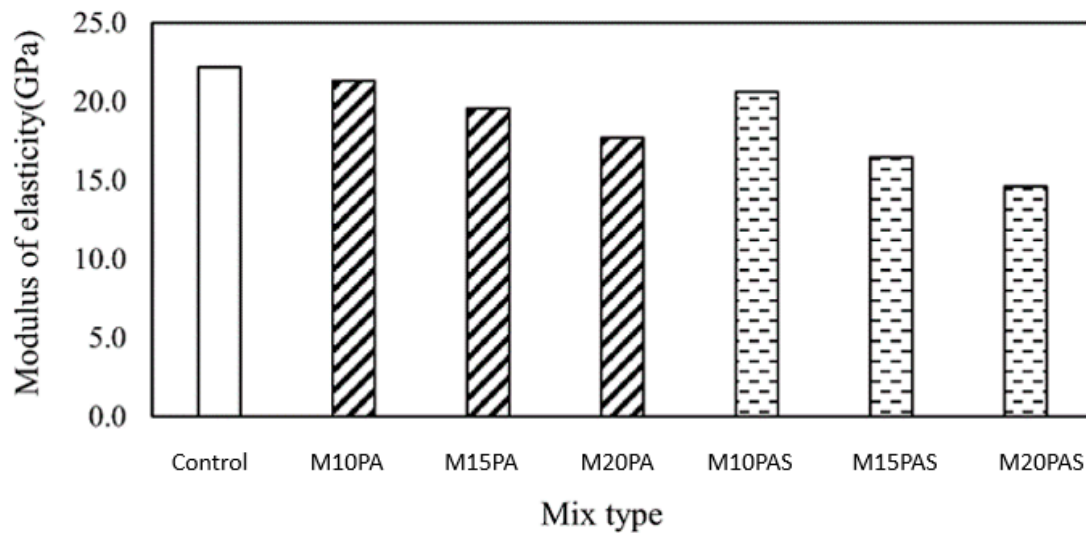


Figure 8. Modulus of elasticity of various mixes.

3.6. Stress–Strain Behavior

An LVDT and strain gauges with a gauge length of 60 mm were used to measure longitudinal strain, while two strain gauges were placed 180 degrees apart in the transverse direction at the middle of the cylinder to measure lateral strain. Figure 9 presents the stress–strain behavior of the concrete blends where it can be observed that with the addition of PA, the brittleness of conventional concrete was reduced. In general, the slope of the curve and the peak strength declined, while the strain corresponding to the peak strength increased with an increase in the PA replacement ratio. In other words, the ductility of PA concrete slightly increased compared to the concrete containing natural aggregates. A similar finding was made by Jansen et al. [39], who employed lightweight fly ash-aggregates and found that as the replacement amount increased, higher ductility was observed with lower CS. The results are also consistent with prior studies [51,80], which found that as the strength increased, the concrete failed at lower strain values. When the replacement level of lightweight expanded polystyrene aggregates increased, failure was more ductile than conventional concrete. Reduced brittleness or ductility is a unique feature of PA concrete that is not exhibited by conventional concrete. This type of concrete is advantageous where dynamic or repeated loading causes failure.

3.7. Lateral Strain and Poisson’s Ratio versus Longitudinal Strain

Lateral versus longitudinal strains of the tested concrete mixes are plotted in Figure 10. It can be noted for concrete mixes with different substitution levels that the control and other concrete mixtures exhibited similar lateral-to-longitudinal strain responses that can be described as bilinear. In general, it can be observed from Figure 10 that the lateral strain increases with an increase in PA content for a given longitudinal strain. Furthermore, compared to the control specimens in which the lateral strain increased abruptly near the peak strength, the rate of lateral strains gradually decreased with the addition of PA. It is also interesting to note that the transition between the two curve portions also occurred earlier for specimens with a higher PA content. In the specimens containing both PA and SF, the addition of SF further reduced the rapid rate of increasing lateral strain and shifted the transition point to a higher strength level. It can be inferred that the addition of PA reduced the brittleness of concrete by exhibiting a relatively smooth transition of higher lateral strains. Similar observations can be carried out for the effect of PA and SF on Poisson’s ratio, as shown in Figure 11. However, it is to be noted that the addition of both PA and SF resulted in a higher lateral strain and Poisson’s ratio compared to concrete with the addition of PA only.

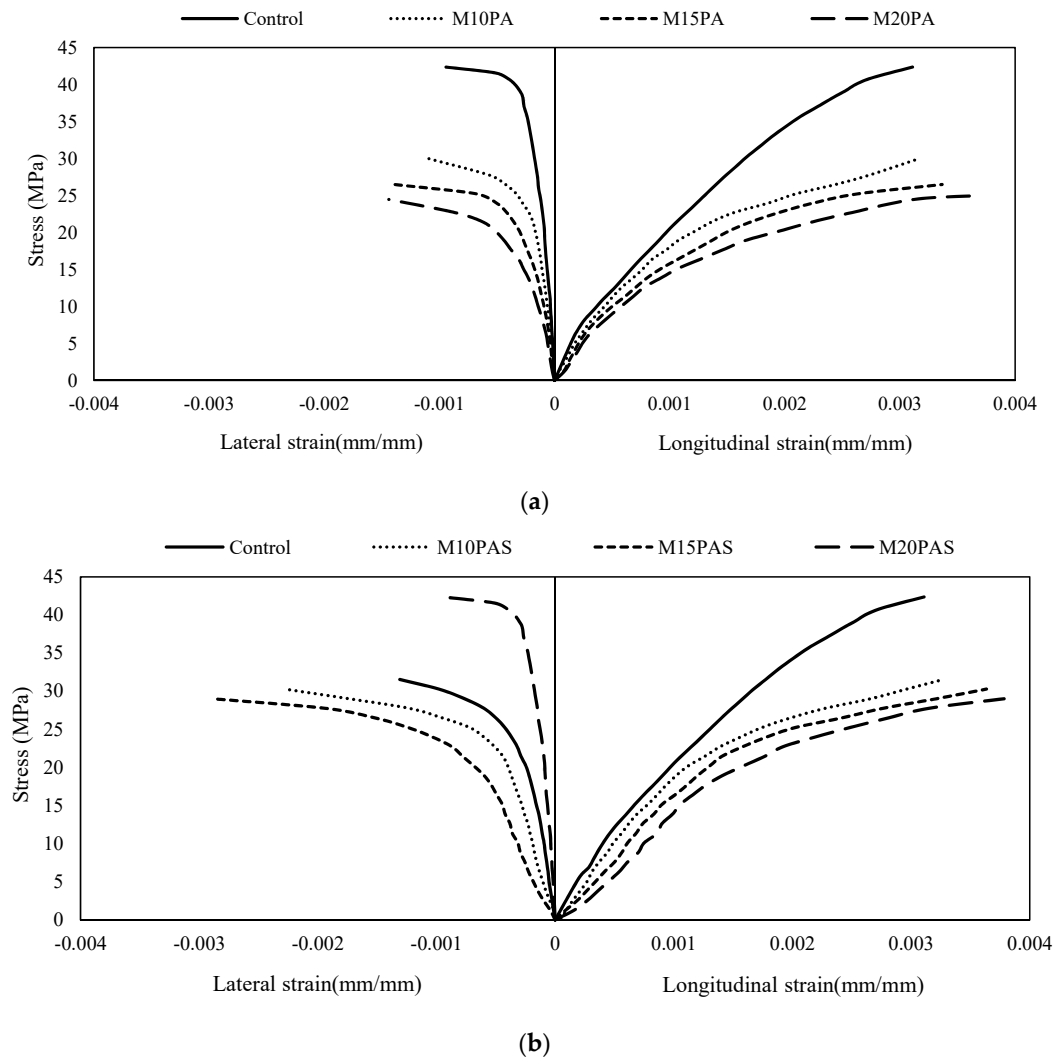


Figure 9. Stress vs. lateral and longitudinal strain relationships for various concrete mixtures: (a) mixtures containing coarse plastic aggregates; (b) mixtures containing coarse plastic aggregates and silica fume.

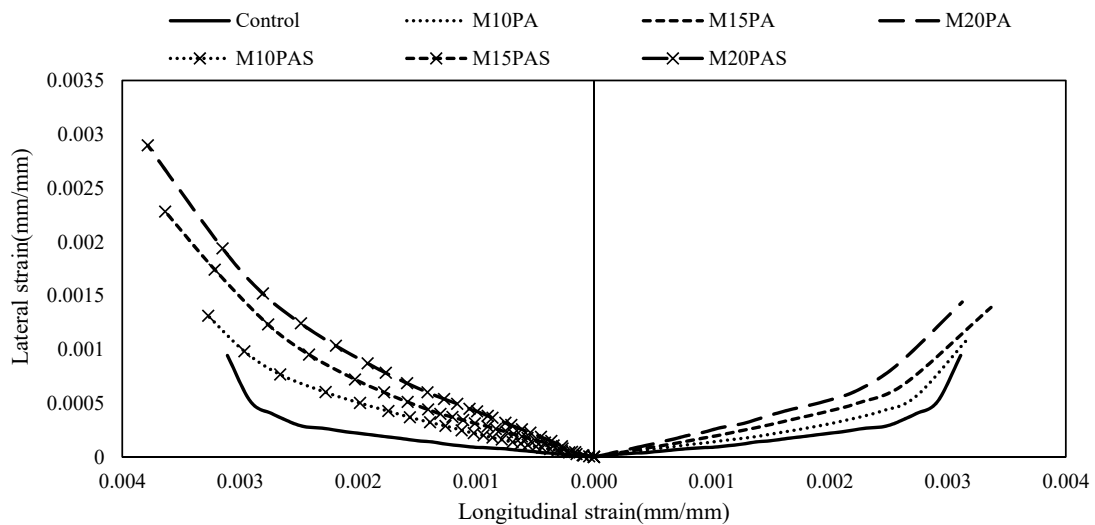


Figure 10. Relationship between the longitudinal and lateral strains for various mixtures.

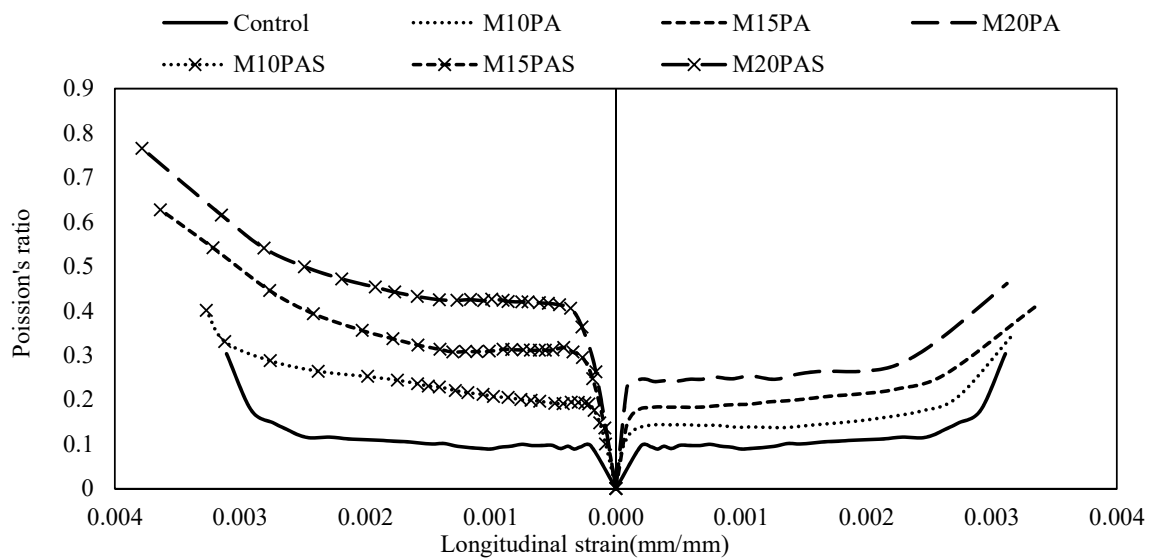


Figure 11. Relationship between the longitudinal strain and Poisson's ratio for various mixtures.

3.8. Correlation between Compressive and Tensile Strengths

Eurocode 2 was used to investigate the STS of concrete [81]. As seen in Equations (2) and (3), the mean indices of STS against any given CS can be determined for normal-strength concrete with a CS of less than 50 MPa using the correlation in Equation (1), where the top and bottom bounds for STS are also given. In these equations, f_{tm} , f_{cm} , $f_{t,min}$, and $f_{t,max}$ represent mean STS, mean CS, minimum, and maximum bounds of STS values, respectively.

$$f_{tm} = 0.3(f_{cm})^{2/3} \quad (1)$$

$$f_{t,min} = 0.7(f_{tm}) \quad (2)$$

$$f_{t,max} = 1.3(f_{tm}) \quad (3)$$

Figure 12 shows the maximum and minimum bounds of STS values, as well as experimental results from current and earlier research, with waste plastic being used as a partial substitute for coarse aggregates [33,37,82]. Without considering the types of plastic, w/c ratios, or the addition of silica fume in this investigation, all measured values from current and past studies fall within the range. In the present research, tensile strength values were determined using suggested equations from many building standards and previous investigations, as indicated in Table 3 and illustrated in Figure 13. The suggested expressions are within Eurocode's minimum and maximum bounds, with Neville's expression [83] at the base and Juki et al.'s [28] at the upper side. It is worth noting that Eurocode defines correction factors for lightweight aggregate concrete tensile strength calculations, indicating a decline in STS against any given CS value. Furthermore, the present research's experimental results reveal that tensile strength values are greater than the conventional concrete values calculated from Equation (1). The New Zealand Standard (NZS:3101:2006) [83] and Neville equations [84] are found to significantly underestimate tensile strength values, with under-predictions ranging from 20% to 32%. The Eurocode, ACI 318-11 [85], Oluokun et al. [86], and Juki et al. [28] equations show a higher correlation with experimental data, with some specimens giving almost precise readings, while others differing by up to 13%. Table 4 displays the experimental-to-projected values ratio as well as the expected tensile strength values.

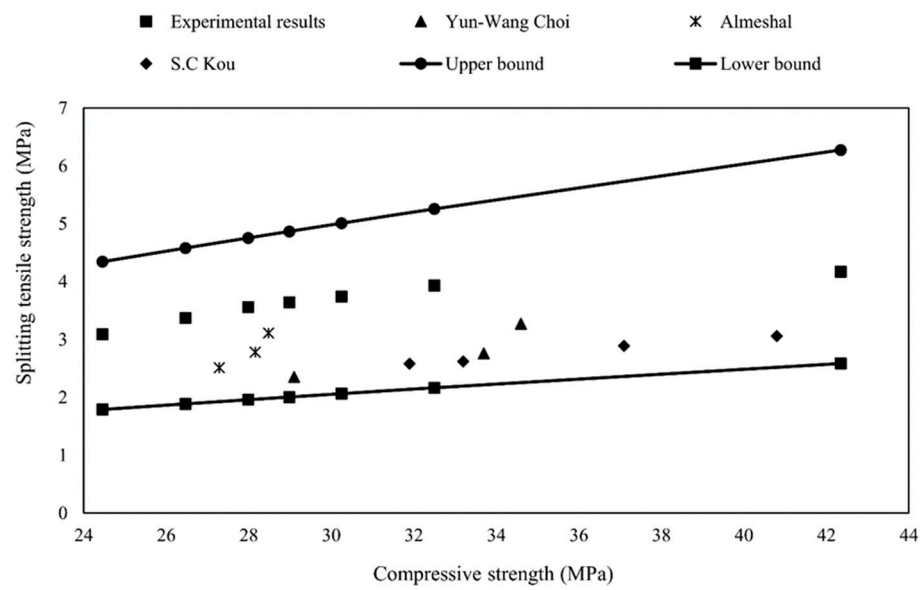


Figure 12. Relationship between compressive and tensile strengths (Yun-Wang Choi [37,38] Almeshal [82], S.C Kou [33]).

Table 3. Suggested model formulae for predicting STS from CS in design codes.

Codes of Practice and Published Works	Expressions	
American Concrete Institute (ACI Committee 318-11)	$f_t = 0.56 * \sqrt{f_c'}$	[85]
New Zealand Standard (NZS: 3101:2006)	$f_t = 0.44 * \sqrt{f_c'}$	[83]
Eurocode	$f_t = 0.3 * f_c^{0.67}$	[81]
Neville	$f_t = 0.23 * f_c^{0.67}$	[84]
Juki et al.	$f_t = 0.214 * f_c^{0.69}$	[28]
Iranian	$f_t = 0.6 * \sqrt{f_c'}$	[87]
Oluokun et al.	$f_t = 0.294 * f_c^{0.69}$	[86]

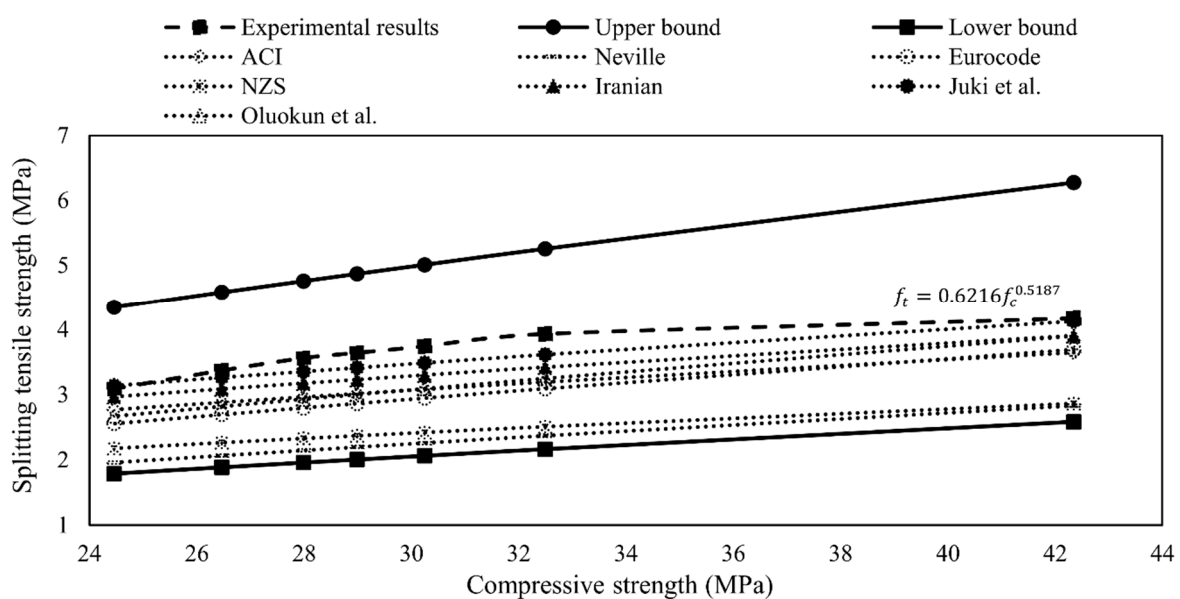


Figure 13. Curves of predicted tensile strength against the compressive strength. (ACI [85], NZS [83], Oluokun et al. [86], Neville [84], Iranian [87], Eurocode [81], Juki et al. [28]).

Table 4. Experimental and analytical STS analysis.

Sample		Control	10-PA	15-PA	20-PA	10-PA-SF	15-PA-SF	20-PA SF
Experimental	f_c (MPa)	42.35	32.50	30.25	28.99	27.99	26.47	24.46
	f_t (MPa)	4.17	3.93	3.74	3.64	3.56	3.37	3.09
	ACI 318-11	3.64	3.19	3.08	3.02	2.96	2.88	2.77
	Neville [84]	2.83	2.37	2.26	2.19	2.14	2.06	1.96
	Juki et al. [28]	2.84	2.36	2.25	2.18	2.13	2.05	1.94
Predicted f_t (MPa)	NZS 3101-2006	2.86	2.51	2.42	2.37	2.33	2.26	2.18
	Oluokun et al. [86]	3.89	3.25	3.09	3.00	2.93	2.82	2.67
	Iranian	3.90	3.42	3.30	3.23	3.17	3.09	2.97
	Euro	3.69	3.09	2.95	2.86	2.80	2.69	2.55
	ACI 318-11	1.15	1.23	1.21	1.21	1.20	1.17	1.12
Experimental/Predicted Value (MPa)	Neville [84]	1.47	1.66	1.65	1.66	1.66	1.64	1.41
	Juki et al. [28]	1.47	1.66	1.66	1.67	1.67	1.64	1.59
	NZS 3101-2006	1.46	1.57	1.55	1.54	1.53	1.49	1.42
	Oluokun et al. [86]	1.07	1.21	1.21	1.21	1.22	1.20	1.16
	Iranian	1.07	1.15	1.13	1.13	1.12	1.09	1.04
	Euro	1.13	1.27	1.27	1.27	1.27	1.25	1.21

3.9. Microscopic Investigation

The shape of plastic and natural aggregates was observed visually and using an optical microscope, as shown in Figures 14 and 15, respectively. It can be observed that the shape of natural and plastic aggregates was quite similar. Visual inspection indicates that plastic aggregates were smooth and somewhat spherical. These particles were placed under an optical compound microscope for detailed visualization of aggregates. It was apparent from the microscopic structure that the plastic aggregate was porous and somewhat spherical. The slices of concrete specimens including PA were also subjected to an optical microscopic analysis, as illustrated in Figure 16. These samples were extracted using a diamond cutter under running water. Figure 16a shows a typical cross-section, while Figure 16b,c present the magnified cross-sections of concrete containing plastic aggregates. Figure 16b depicts the hydrophobic nature of the plastic aggregates and the amalgamation of cement matrix around plastic aggregates. Figure 16c shows the bond between the PA and cement matrix.



Figure 14. Aggregate visual inspection: (a) natural aggregate; (b) plastic aggregate.

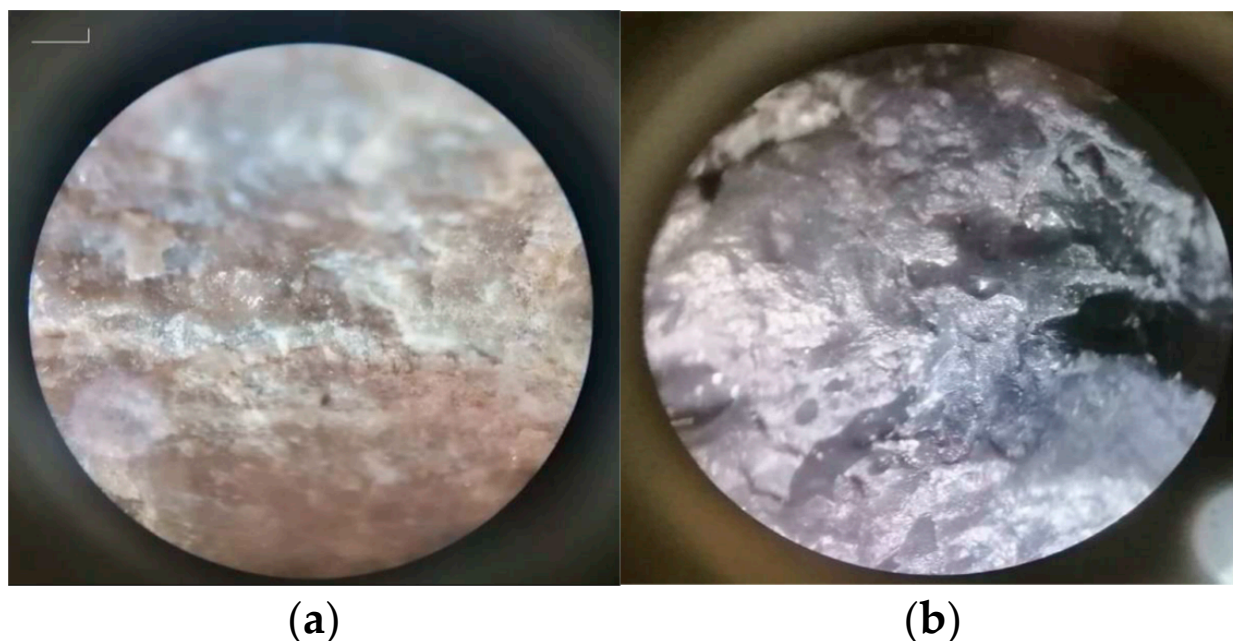


Figure 15. Aggregate optical microscopic image: (a) natural aggregate; (b) plastic aggregate.

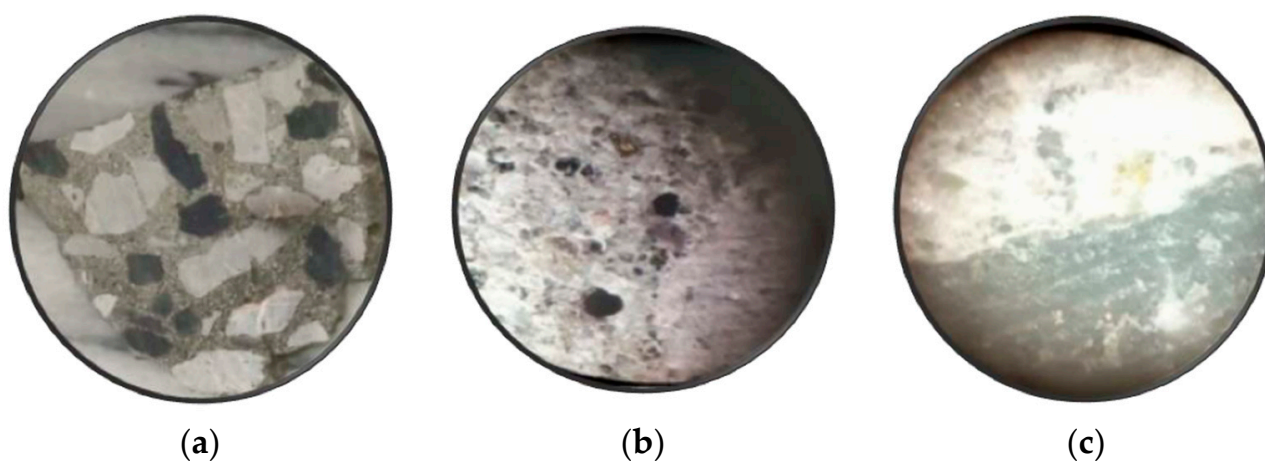


Figure 16. Optical microscopic image of the concrete slice: (a) typical cross-section of plastic aggregate concrete; (b) microscopic view of plastic aggregate concrete; (c) bond between plastic aggregate and cement matrix.

Figure 17 shows the cement matrix's crack width and bond with conventional and plastic aggregates. The crack width of the natural aggregate was 1 μm , while for the plastic aggregate, it was 8, 11 and 24 μm . These SEM images exhibited a weak bond between the cement matrix and plastic aggregate, which may explain the reason behind the strength deterioration of the concrete mixes containing plastic aggregates compared to natural aggregates. This result also indicates that the concrete containing PA was porous in nature, which can also be another reason for the lower strength. EDS was also taken at the plastic aggregate in the concrete mix, and the spectrum showed that calcium was present in it (Figure 18). XRD of the plastic aggregate was also performed, showing the chemical composition of the plastic aggregate. Calcium was present in the plastic aggregate, as shown in Figure 19.

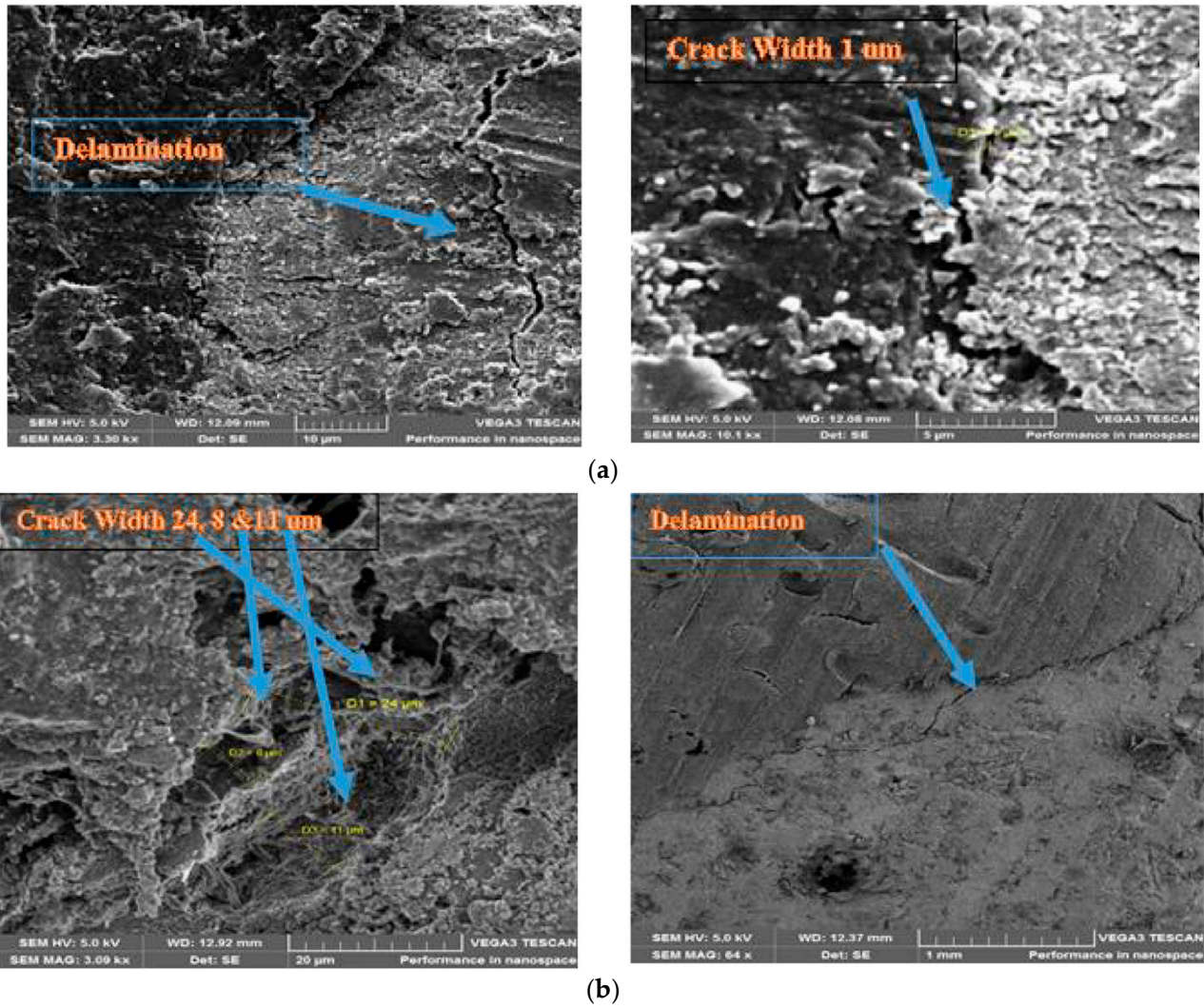


Figure 17. The crack width and bond pattern of natural and plastic aggregates with cement matrix: (a) natural aggregate concrete; (b) plastic aggregate concrete.

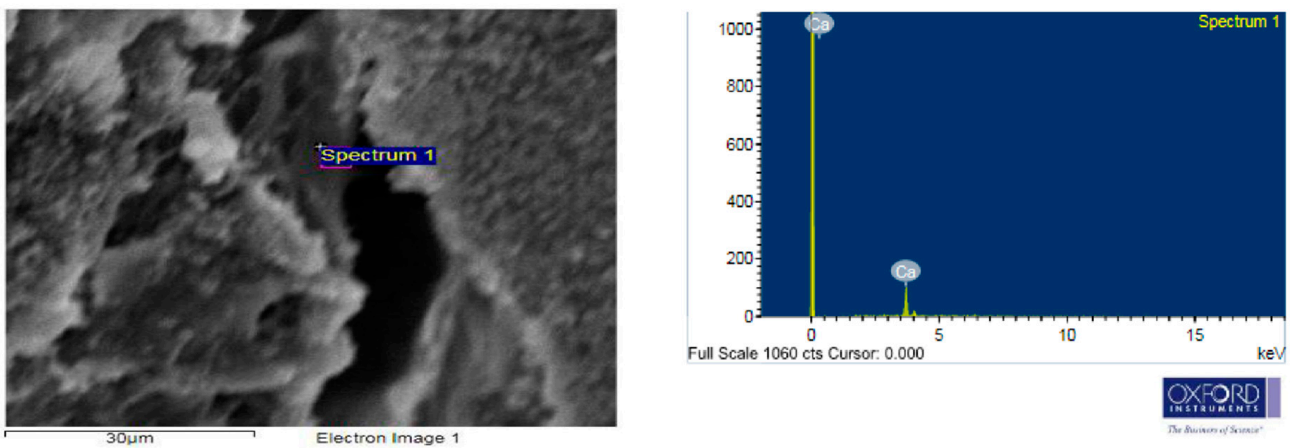


Figure 18. EDS spectrum.

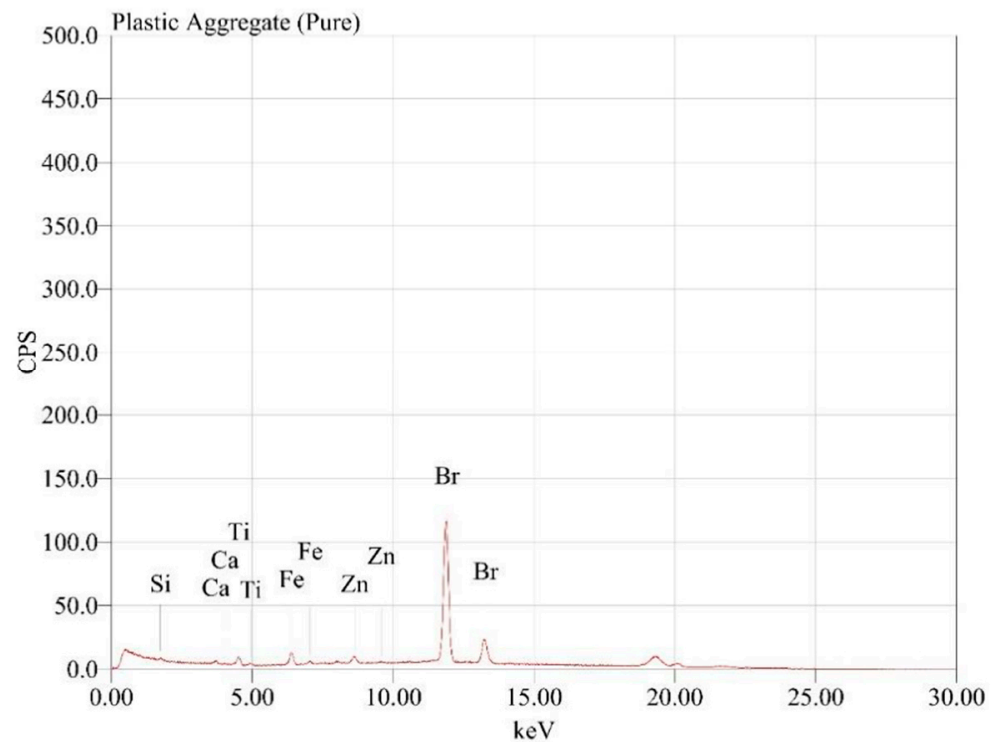


Figure 19. XRD of plastic aggregate.

4. Thermal Performance Analysis

Energy preservation is currently one of the prime concerns, and special efforts are being made in the construction sector to select energy-efficient materials to conserve as much energy as possible. The thermal performance of concrete made with natural and plastic aggregates was investigated both indoors and outdoors in the present research. The test setup used in a previous study conducted by the authors of [51] was also employed in the current work. For this purpose, concrete slabs of $203 \times 203 \times 38$ mm were cast with the same mix design as discussed in Section 2. Two mixes, i.e., control and 20% PA, SF, were employed to prepare the slab specimens. The motive was to observe the maximum temperature differential of the mixes containing minimum and maximum plastic aggregate and silica fume content. The thermal performance test was conducted after 28 days of curing.

4.1. Indoor Thermal Performance

Figure 20 illustrates the test setup used to assess the concrete slabs' indoor thermal performance. The test assembly consisted of a wooden box comprised of two chambers (upper and lower), while the slab specimen rested between both chambers. The dimensions of both compartments are shown in Figure 20. The upper chamber was equipped with a 300 W coil for providing heat to the slab. The sides of the test assembly were sealed with aluminum foil to prevent any heat loss. The temperature of the slab specimens from the top and bottom surfaces and the lower chamber was determined using sensors. The experiment started at ambient temperature and continued until the temperature of the upper chamber reached 130°C . Afterward, the coil was turned off, and the cooling of the upper chamber took place until room temperature was achieved. The temperature curves obtained by sensor 3, as presented in Figure 21, demonstrate the variation of heat transfer for both the tested slab specimens, as the difference between the temperature increases for both specimens was evident. Although it can be observed that the ascending curve of temperature rise detected at the bottom of both the slab specimens followed an almost similar slope, the slab specimen containing plastic aggregates exhibited better thermal

performance compared to the control specimen. A notable difference was recorded between the temperature of both specimens in the plateau region. The concrete incorporating plastic aggregates and silica fume attained a $1.75\text{ }^{\circ}\text{C}$ (4.2%) lower temperature at the base of the slab, showing better thermal performance. Furthermore, the difference between the two curves widened up in the descending portion, and the plastic aggregate concrete attained room temperature significantly earlier than the control slab specimen.

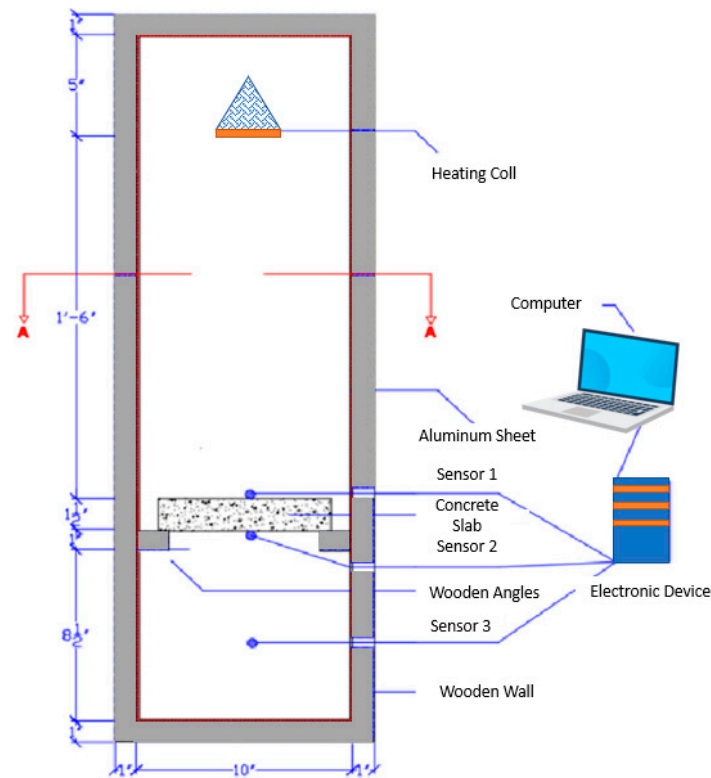


Figure 20. Setup for indoor thermal performance test [51]: front view of indoor thermal performance setup.

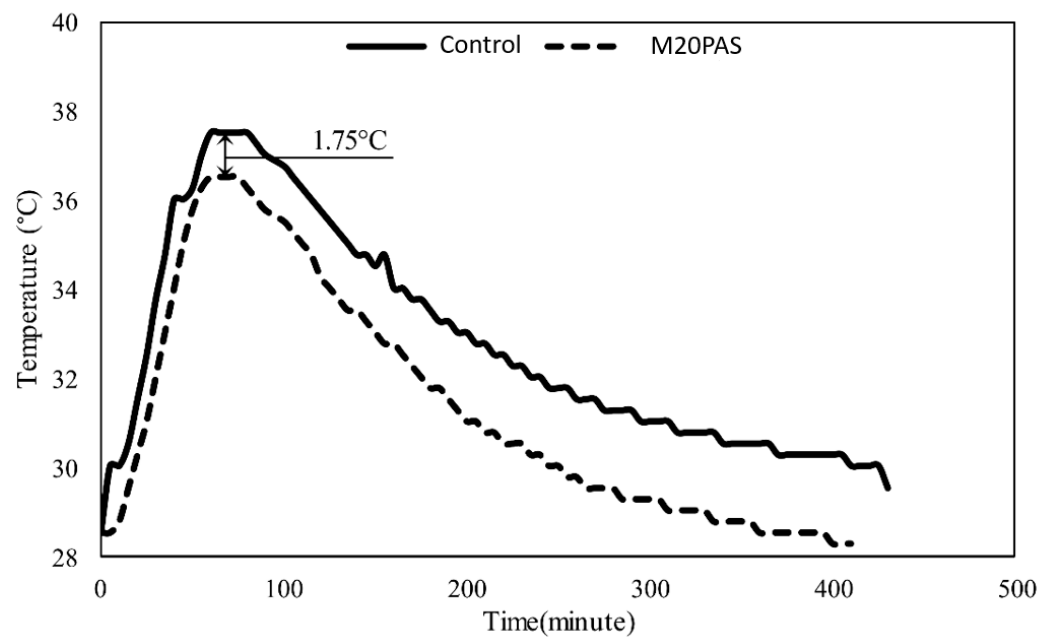


Figure 21. Indoor thermal performance of slab specimens.

4.2. Outdoor Thermal Performance

The test assembly employed to assess the outdoor thermal performance of both concrete slab specimens is shown in Figure 22. The wooden box used in this test consisted of only the lower chamber, and the slab specimens were placed on top of it. As demonstrated in Figure 22, the chamber dimensions were kept the same as those used in the indoor thermal performance experiment. Sunlight was used as the heating source. Temperature sensors attached to the inner and outer surfaces of the slab specimens were connected to a computer system to record the temperature at regular intervals. The temperature curves obtained by sensor 3 are shown in Figure 23, where it can be observed that the outdoor thermal performance of both slab specimens was quite similar to the indoor thermal performance. The concrete incorporating plastic aggregates and silica fume exhibited a 2.5 °C (8%) lower temperature at the bottom surface of the specimen compared to the control specimen, indicating superior thermal performance. The descending curve illustrated a faster cooling rate of the concrete containing plastic aggregates and silica fume, which took 40% less time to achieve room temperature than the control specimen. The thermal efficiency of plastic aggregate concrete is evident from the indoor and outdoor thermal performance tests and can be a viable option when selecting energy-efficient building materials.

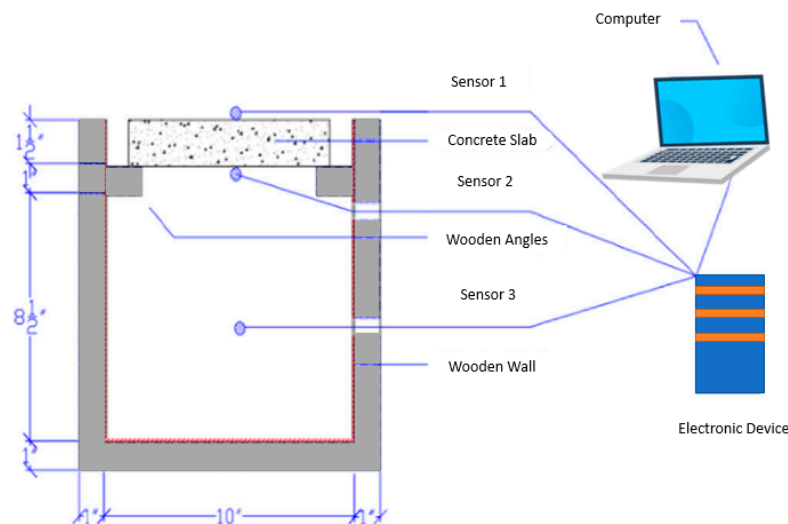


Figure 22. Setup for outdoor thermal performance test [51]: front view of outdoor thermal performance setup.

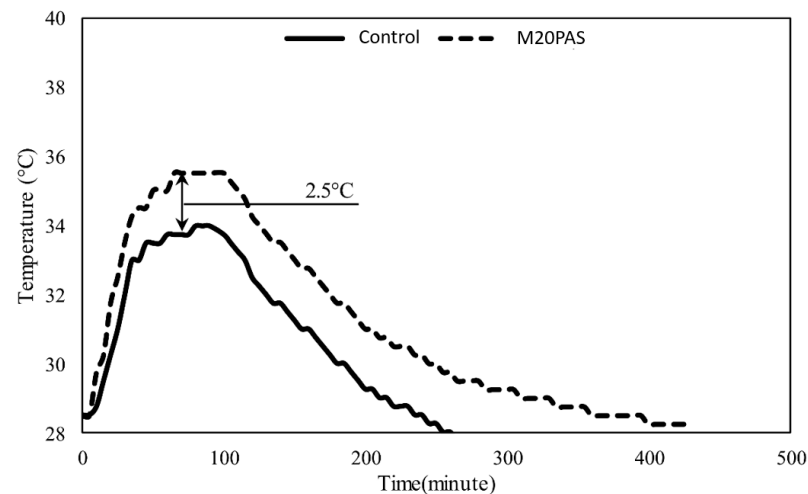


Figure 23. Outdoor thermal performance of slab specimens.

4.3. Thermo-Gravimetric Analysis

The thermal stability of the control and 20% PA, SF concrete samples was investigated using thermo-gravimetric analysis (TGA). Test samples were taken from the center of cylindrical cores, which were then powdered to an 80-micron particle size. The test samples were weighed before placing them in a furnace where the test samples were exposed to elevated temperatures up to 800 °C. Figure 24 demonstrates the percent weight loss for both test samples over the temperature range. A similar weight loss trend can be observed for both test samples up to 300 °C due to the evaporation of many hydrates, such as C-S-H, carbo-aluminates, ettringite, etc. Contrary to the control sample, the 20% PA, SF concrete sample exhibited a significant weight loss between 300 and 480 °C that can be attributed to the evolution of butadiene monomer and styrene in plastic aggregates at around 340 °C and 350 °C, respectively, as observed in the past research conducted on pure ABS plastic [88,89]. The control sample experienced substantial weight loss in the temperature range of 600–800 °C, which can be due to the decarbonation of calcium carbonate that is primarily found in clinker [87,90,91]. The drastic weight loss due to plastic aggregates resulted in an overall weight loss of around 89% in the 20% PA, SF concrete sample compared to a 29% weight reduction for the control sample, as indicated in Table 5.

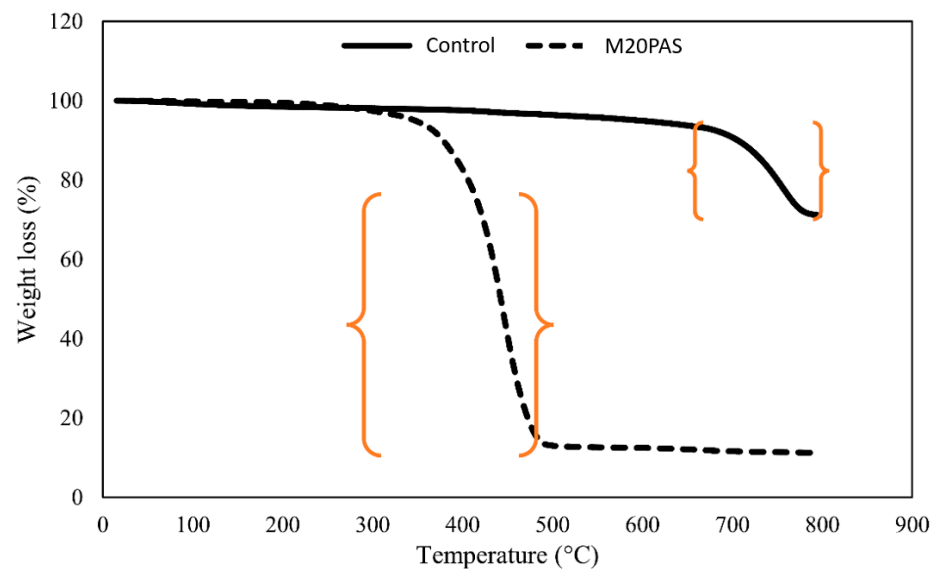


Figure 24. Thermo-gravimetric analysis results.

Table 5. Weight reduction observed during TGA.

Temperature °C	0–180	180–300	300–470	470–600	600–700	700–800
Control Specimen	1.41%	1.92%	3.27%	5.06%	9.23%	28.91%
M20PAS	0.41%	2.57%	78.37%	87.55%	88.42%	88.94%

5. Conclusions

According to this study, PA influenced the properties of concrete, such as fresh and dry density, stress–strain behavior, Poisson’s ratio, and E-value. The thermal performance of concrete incorporating PA was also investigated. PA was used to replace natural coarse aggregates at replacement levels of 10, 15, and 20%, with and without SF incorporation as a cement substitution at an equivalent replacement percentage. The following conclusions are drawn:

- The addition of PA in concrete enhanced the slump due to the non-absorbent and relatively spherical shape of the PA. The slump of concrete mixes increased from 25 mm to 155 mm for the control and a 20% replacement of coarse aggregates with PA, respectively.

- The integration of PA into concrete decreased the fresh and dry density of concrete blends to a maximum of 9.7% and 11.25%, respectively. The maximum reduction was observed for a 20% addition of PA with and without SF. This reduction in density could be attributed to the lower densities of plastic aggregates and silica fume, i.e., 760 kg/m³ and 784 kg/m³, respectively, compared to 1518 kg/m³ and 1440 kg/m³ of natural aggregates and cement, respectively.
- The use of PA decreased the CS and STS of concrete by 31.5 to 42.2% and 31.8 to 36.92%, correspondingly, for substitution levels of 10 to 20%. Furthermore, the integration of SF as a substitution for cement by 10, 15, and 20% led to a significantly lower reduction in CS and STS, although the PA content substitution was the same. CS reductions for the replacement (10, 15, and 20%) of PA and SF were found to be 25.53%, 28.55%, and 31.5%, respectively. Similarly, the STS reductions for the replacement (10, 15, and 20%) of PA and SF were found to be 24.11%, 25.53%, and 32.26%, respectively. The results show that by integrating SF at the same replacement percentage as PA, the reduction in CS and STS was lower as compared to replacing PA only.
- The stress–strain relationship demonstrated that in comparison to the control mix, samples with PA exhibited greater failure strain values and a more ductile response. However, the low strength of the PA concrete mixes might also be attributed to the increase in strain values. The E-value was observed to decline as the percentage of PA increased, with a maximum reduction of 42.23%. However, at the maximum replacement of PA and SF, the reduction in the modulus of elasticity was 31.53%, which was 25.53% lower than the only 20% substitution of PA. This shows that the incorporation of SF reduced the E-value.
- The relationship between the experimental CS and STS values, as identified by CEB-FIP, was found to be within the maximum and minimum bound and identical to prior PA investigations.
- The plastic aggregates were observed to be porous, smooth, and somewhat spherical in shape. The crack width of the natural aggregate was 1 µm, while for the plastic aggregate, it was 8, 11 and 24 µm.
- Both in indoor and outdoor thermal performance tests, concrete with plastic aggregates outperformed concrete without PA in terms of thermal insulation, reducing thermal conductivity by more than 2.5%.

Future Recommendations

The overall evaluation shows the importance of a sustainable concrete mixture with equivalent fresh and mechanical properties as well as better thermal performance. Future studies need to focus on enhancing the mechanical properties of plastic aggregate concrete while effectively increasing the plastic aggregate content in the concrete mixtures. This can be explored by carrying out the surface treatment of plastic aggregates to improve the bond between the cement paste matrix and the plastic aggregates. Moreover, the plastic aggregate incorporation can be explored at the structural member level, such as in beams and columns.

Author Contributions: Conceptualization, P.S., M.I.Q., T.M. and S.S. (Suniti Suparp); Methodology, P.S., M.I.Q., A.N. and T.M.; Software, K.A. and M.I.Q.; Validation, M.I.Q., T.M. and S.S. (Suniti Suparp); Formal analysis, M.I.Q.; Investigation, S.S. (Shahzad Saleem); Resources, S.S. (Shahzad Saleem), A.M. and M.W.M.; Data curation, K.A., S.S. (Shahzad Saleem), A.M. and M.W.M.; Writing—original draft, P.S., A.N., A.M., M.W.M. and S.S. (Suniti Suparp); Writing—review & editing, K.A., P.S., A.N., M.W.M. and S.S. (Suniti Suparp); Supervision, S.S. (Shahzad Saleem) and A.M.; Project administration, S.S. (Shahzad Saleem) and A.N. All authors have read and agreed to the published version of the manuscript.

Funding: The research funding was provided by Thailand Science Research and Innovation (TSRI) and National Science Research and Innovation Fund (NSRF) (Fundamental Fund: Grant No. 051/2566).

Acknowledgments: The authors are grateful to Thailand Science Research and Innovation (TSRI) and National Science Research and Innovation Fund (NSRF) for providing research grant (Fundamental Fund: Grant No. 051/2566).

Conflicts of Interest: The authors declare no conflict of interest.

References

1. Monteiro, P.J.; Miller, S.A.; Horvath, A. Towards sustainable concrete. *Nat. Mater.* **2017**, *16*, 698–699. [CrossRef] [PubMed]
2. Saikia, N.; De Brito, J. Mechanical properties and abrasion behaviour of concrete containing shredded PET bottle waste as a partial substitution of natural aggregate. *Constr. Build. Mater.* **2014**, *52*, 236–244. [CrossRef]
3. Haas, K. *Lifecycle Cost and Performance of Plastic Pipelines in Modern Water Infrastructure*; University California: Davis, CA, USA, 2012.
4. Silva, R.V.; Jiménez, J.R.; Agrela, F.; de Brito, J. Real-scale applications of recycled aggregate concrete. In *New Trends in Eco-Efficient and Recycled Concrete*; Elsevier: Amsterdam, The Netherlands, 2019; pp. 573–589.
5. Curry-Lindahl, K. United Nations Environment Programme. In *EARTHCARE: Global Protection of Natural Areas*; Routledge: England, UK, 2019; pp. 740–753.
6. Ullah, Z.; Qureshi, M.I.; Ahmad, A.; Khan, S.U.; Javaid, M.F. An experimental study on the mechanical and durability properties assessment of E-waste concrete. *J. Build. Eng.* **2021**, *38*, 102177. [CrossRef]
7. Allujami, H.M.; Abdulkareem, M.; Jassam, T.M.; Al-Mansob, R.A.; Ibrahim, A.; Ng, J.L.; Yam, H.C. Mechanical properties of concrete containing recycle concrete aggregates and multi-walled carbon nanotubes under static and dynamic stresses. *Case Stud. Constr. Mater.* **2022**, *17*, e01651. [CrossRef]
8. Allujami, H.M.; Abdulkareem, M.; Jassam, T.M.; Al-Mansob, R.A.; Ng, J.L.; Ibrahim, A. Nanomaterials in recycled aggregates concrete applications: Mechanical properties and durability. A review. *Cogent Eng.* **2022**, *9*, 2122885. [CrossRef]
9. Arabiyat, S.; Katkhuda, H.; Shatarat, N. Influence of using two types of recycled aggregates on shear behavior of concrete beams. *Constr. Build. Mater.* **2021**, *279*, 122475. [CrossRef]
10. Abdollahnejad, Z.; Mastali, M.; Falah, M.; Luukkonen, T.; Mazari, M.; Illikainen, M. Construction and demolition waste as recycled aggregates in alkali-activated concretes. *Materials* **2019**, *12*, 4016. [CrossRef]
11. Batayneh, M.; Marie, I.; Asi, I. Use of selected waste materials in concrete mixes. *Waste Manag.* **2007**, *27*, 1870–1876. [CrossRef]
12. Solahuddin, B.A.; Yahaya, F.M. Properties of concrete containing shredded waste paper as an additive. *Mater. Today Proc.* **2022**, *51*, 1350–1354. [CrossRef]
13. Joyklad, P.; Ali, N.; Chaiyasarn, K.; Poovarodom, N.; Yooprasertchai, E.; Maqbool, H.M.; Hussain, Q. Improvement of stress-strain behavior of brick-waste aggregate concrete using low-cost FCSM composites. *Constr. Build. Mater.* **2022**, *351*, 128946. [CrossRef]
14. Batayneh, M.K.; Marie, I.; Asi, I. Promoting the use of crumb rubber concrete in developing countries. *Waste Manag.* **2008**, *28*, 2171–2176. [CrossRef]
15. Plastic Production Is on the Rise Worldwide But Declining in Europe. 2019. Available online: <https://www.brinknews.com/quick-take/plastic-production-on-the-rise-worldwide-declining-in-europe/> (accessed on 20 March 2023).
16. Saikia, N.; De Brito, J. Use of plastic waste as aggregate in cement mortar and concrete preparation: A review. *Constr. Build. Mater.* **2012**, *34*, 385–401. [CrossRef]
17. Kershaw, P.; Katsuhiko, S.; Lee, S.; Woodring, D. *Plastic Debris in the Ocean*; United Nations Environment Programme: Nairobi, Kenya, 2011.
18. Sesini, M. *The Garbage Patch in the Oceans: The Problem and Possible Solutions*; Columbia Univ.: New York, NY, USA, 2011.
19. Ferrotto, M.F.; Asteris, P.G.; Borg, R.P.; Cavaleri, L. Strategies for waste recycling: The mechanical performance of concrete based on limestone and plastic waste. *Sustainability* **2022**, *14*, 1706. [CrossRef]
20. Mohammed, T.K.; Hama, S.M. Mechanical properties, impact resistance and bond strength of green concrete incorporating waste glass powder and waste fine plastic aggregate. *Innov. Infrastruct. Solut.* **2022**, *7*, 1–12. [CrossRef]
21. Faraj, R.H.; Ahmed, H.U.; Sherwani, A.F.H. Fresh and mechanical properties of concrete made with recycled plastic aggregates. In *Handbook of Sustainable Concrete and Industrial Waste Management*; Elsevier: Amsterdam, The Netherlands, 2022; pp. 167–185.
22. Ahmad, F.; Jamal, A.; Mazher, K.M.; Umer, W.; Iqbal, M. Performance evaluation of plastic concrete modified with E-waste plastic as a partial replacement of coarse aggregate. *Materials* **2021**, *15*, 175. [CrossRef]
23. Albano, C.; Camacho, N.; Hernandez, M.; Matheus, A.; Gutierrez, A. Influence of content and particle size of waste pet bottles on concrete behavior at different w/c ratios. *Waste Manag.* **2009**, *29*, 2707–2716. [CrossRef]
24. Hannawi, K.; Kamali-Bernard, S.; Prince, W. Physical and mechanical properties of mortars containing PET and PC waste aggregates. *Waste Manag.* **2010**, *30*, 2312–2320. [CrossRef]
25. Rahmani, E.; Dehestani, M.; Beygi, M.H.A.; Allahyari, H.; Nikbin, I.M. On the mechanical properties of concrete containing waste PET particles. *Constr. Build. Mater.* **2013**, *47*, 1302–1308. [CrossRef]
26. Khan, M.I.; Sutanto, M.H.; Napiyah, M.B.; Khan, K.; Rafiq, W. Design optimization and statistical modeling of cementitious grout containing irradiated plastic waste and silica fume using response surface methodology. *Constr. Build. Mater.* **2021**, *271*, 121504. [CrossRef]

27. Jain, A.; Siddique, S.; Gupta, T.; Jain, S.; Sharma, R.K.; Chaudhary, S. Evaluation of concrete containing waste plastic shredded fibers: Ductility properties. *Struct. Concr.* **2021**, *22*, 566–575. [[CrossRef](#)]
28. Juki, M.I.; Awang, M.; Annas, M.M.K.; Boon, K.H.; Othman, N.; Roslan, M.A.; Khalid, F.S. Relationship between compressive, splitting tensile and flexural strength of concrete containing granulated waste Polyethylene Terephthalate (PET) bottles as fine aggregate. In *Advanced Materials Research*; Trans Tech Publ.: Stafa-Zurich, Switzerland, 2013; pp. 356–359.
29. Sabaa, B.; Ravindrarajah, R.S. Engineering properties of lightweight concrete containing crushed expanded polystyrene waste. In *Proceedings of the Symposium MM: Advances in Materials for Cementitious Composites*, Boston, MA, USA, 1–5 December 1997; pp. 1–3.
30. Khan, K.; Ahmad, W.; Amin, M.N.; Nazar, S. Nano-silica-modified concrete: A bibliographic analysis and comprehensive review of material properties. *Nanomaterials* **2022**, *12*, 1989. [[CrossRef](#)] [[PubMed](#)]
31. Ahmad, F.; Qureshi, M.I.; Ahmad, Z. Influence of nano graphite platelets on the behavior of concrete with E-waste plastic coarse aggregates. *Constr. Build. Mater.* **2022**, *316*, 125980. [[CrossRef](#)]
32. Ismail, Z.Z.; Al-Hashmi, E.A. Use of waste plastic in concrete mixture as aggregate replacement. *Waste Manag.* **2008**, *28*, 2041–2047. [[CrossRef](#)] [[PubMed](#)]
33. Kou, S.C.; Lee, G.; Poon, C.S.; Lai, W.L. Properties of lightweight aggregate concrete prepared with PVC granules derived from scraped PVC pipes. *Waste Manag.* **2009**, *29*, 621–628. [[CrossRef](#)] [[PubMed](#)]
34. Tang, W.C.; Lo, Y.; Nadeem, A. Mechanical and drying shrinkage properties of structural-graded polystyrene aggregate concrete. *Cem. Concr. Compos.* **2008**, *30*, 403–409. [[CrossRef](#)]
35. Wang, R.; Meyer, C. Performance of cement mortar made with recycled high impact polystyrene. *Cem. Concr. Compos.* **2012**, *34*, 975–981. [[CrossRef](#)]
36. Herki, B.A.; Khatib, J.M.; Negim, E.M. Lightweight concrete made from waste polystyrene and fly ash. *World Appl. Sci. J.* **2013**, *21*, 1356–1360.
37. Choi, Y.-W.; Moon, D.-J.; Chung, J.-S.; Cho, S.-K. Effects of waste PET bottles aggregate on the properties of concrete. *Cem. Concr. Res.* **2005**, *35*, 776–781. [[CrossRef](#)]
38. Choi, Y.W.; Moon, D.J.; Kim, Y.J.; Lachemi, M. Characteristics of mortar and concrete containing fine aggregate manufactured from recycled waste polyethylene terephthalate bottles. *Constr. Build. Mater.* **2009**, *23*, 2829–2835. [[CrossRef](#)]
39. Jansen, D.C.; Kiggins, M.L.; Swan, C.W.; Malloy, R.A.; Kashi, M.G.; Chan, R.A.; Javdekar, S.; Siegal, C.; Weingram, J. Lightweight fly ash-plastic aggregates in concrete. *Transp. Res. Rec.* **2001**, *1775*, 44–52. [[CrossRef](#)]
40. Malloy, R.; Desai, N.; Wilson, C.; Swan, C.; Jansen, D.; Kashi, M. High carbon fly ash/mixed thermoplastic aggregate for use in lightweight concrete (859). In *Technical Papers of the Annual Technical Conference-Society of Plastics Engineers Incorporated*; 2001; pp. 2743–2752.
41. Slabaugh, S.; Swan, C.; Malloy, R. Development and properties of foamed synthetic Lightweight Aggregates. In *Proceedings of the World of Coal Ash Conference*, Covington, KY, USA, 7–10 May 2007.
42. Panyakapo, P.; Panyakapo, M. Reuse of thermosetting plastic waste for lightweight concrete. *Waste Manag.* **2008**, *28*, 1581–1588. [[CrossRef](#)]
43. Assaad, J.J.; Khatib, J.M.; Ghanem, R. Bond to bar reinforcement of PET-modified concrete containing natural or recycled coarse aggregates. *Environments* **2022**, *9*, 8. [[CrossRef](#)]
44. Saxena, R.; Siddique, S.; Gupta, T.; Sharma, R.K.; Chaudhary, S. Impact resistance and energy absorption capacity of concrete containing plastic waste. *Constr. Build. Mater.* **2018**, *176*, 415–421. [[CrossRef](#)]
45. Najaf, E.; Abbasi, H. Using recycled concrete powder, waste glass powder, and plastic powder to improve the mechanical properties of compacted concrete: Cement elimination approach. *Adv. Civ. Eng.* **2022**, *2022*, 9481466. [[CrossRef](#)]
46. Hossain, M.S.; Penmethsa, K.K.; Hoyos, L. Permeability of municipal solid waste in bioreactor landfill with degradation. *Geotech. Geol. Eng.* **2009**, *27*, 43–51. [[CrossRef](#)]
47. Prasanna, P.K.; Rao, M.K. Strength variations in concrete by using E-waste as coarse aggregate. *Int. J. Educ. Appl. Res.* **2014**, *4*.
48. Akram, A.; Sasidhar, C.; Pasha, K.M. E-waste management by utilization of E-plastics in concrete mixture as coarse aggregate replacement. *Int. J. Innov. Res. Sci. Eng. Technol.* **2015**, *4*, 5087–5095.
49. Alagusankareswari, K.; Kumar, S.S.; Vignesh, K.B.; Niyas, K.A.H. An experimental study on e-waste concrete. *Indian J. Sci. Technol.* **2016**, *9*, 1–5. [[CrossRef](#)]
50. Javaid, M.F.; Qureshi, M.I.; Saleem, S. Effect of temperature on behavior of concrete with E-waste as partial replacement of aggregates. In *Proceedings of the 3rd Pak-Turk International Conference Proceedings*, Topi, Pakistan, 9–10 June 2020; Ghulam Ishaq Khan Institute of Engineering Sciences & Technology: Topi, Pakistan, 2020; pp. 9–10.
51. Ali, K.; Qureshi, M.I.; Saleem, S.; Khan, S.U. Effect of waste electronic plastic and silica fume on mechanical properties and thermal performance of concrete. *Constr. Build. Mater.* **2021**, *285*, 122952. [[CrossRef](#)]
52. ASTM C127; Standard Test Method for Relative Density (Specific Gravity) and Absorption of Coarse Aggregate. ASTM International: West Conshohocken, PA, USA, 2015.
53. ASTM C136/C136M; Standard Test Method for Sieve Analysis of Fine and Coarse Aggregates. ASTM International: West Conshohocken, PA, USA, 2014; pp. 1–5. Available online: www.astm.org (accessed on 20 March 2023).
54. C136-14, C136/C136M-14, C136-14; Standard Test Method for Sieve Analysis of Fine and Coarse Aggregates. ASTM International: West Conshohocken, PA, USA, 2014.

55. ASTM C1437; Standard Test Method for Flow of Hydraulic Cement Mortar. ASTM International: West Conshohocken, PA, USA, 2013.
56. ASTM C138/C138M; Standard Test Method for Density (Unit Weight), Yield, and Air Content (Gravimetric) of Concrete. ASTM International: West Conshohocken, PA, USA, 2017. Available online: <https://compass-astm-org.proxy.findit.dtu.dk/download/C138C138M.15171.pdf> (accessed on 20 March 2023).
57. BS EN 12390-7; Testing Hardened Concrete: Density of Hardened Concrete. Br Stand Institution: London, UK, 2009.
58. BS EN 12390-6; Testing Hardened Concrete. Tensile Splitting Strength of Test Specimens. Br Stand Institution: London, UK, 2009.
59. ASTM C39/C39M; Standard Test Method for Compressive Strength of Cylindrical Concrete Specimens. ASTM International: West Conshohocken, PA, USA, 2018.
60. ASTM C469/C469M; Standard Test Method for Static Modulus of Elasticity and Poisson's Ratio of Concrete in Compression. ASTM International: West Conshohocken, PA, USA, 2014.
61. Silva, R.V.; de Brito, J.; Saikia, N. Influence of curing conditions on the durability-related performance of concrete made with selected plastic waste aggregates. *Cem. Concr. Compos.* **2013**, *35*, 23–31. [[CrossRef](#)]
62. Hadipramana, J.; Mokhatar, S.N.; Samad, A.A.A.; Hakim, N.F.A. An exploratory compressive strength of concrete containing modified artificial Polyethylene aggregate (MAPEA). In *IOP Conference Series: Materials Science and Engineering*; IOP Publishing: Bristol, UK, 2016; p. 12065.
63. Ghernouti, Y.; Rabeih, B.; Safi, B.; Chaid, R. Use of recycled plastic bag waste in the concrete. *J. Int. Sci. Publ. Mater. Methods Technol.* **2011**, *8*, 480–487.
64. Al-Manaseer, A.A.; Dalal, T.R. Concrete containing plastic aggregates. *Concr. Int.* **1997**, *19*, 47–52.
65. Farahani, J.N.; Shafigh, P.; Alsubari, B.; Shahnazari, S.; Mahmud, H.B. Engineering properties of lightweight aggregate concrete containing binary and ternary blended cement. *J. Clean. Prod.* **2017**, *149*, 976–988. [[CrossRef](#)]
66. Fraj, A.B.; Kismi, M.; Mounanga, P. Valorization of coarse rigid polyurethane foam waste in lightweight aggregate concrete. *Constr. Build. Mater.* **2010**, *24*, 1069–1077. [[CrossRef](#)]
67. Mathew, P.; Varghese, S.; Paul, T.; Varghese, E. Recycled plastics as coarse aggregate for structural concrete. *Int. J. Innov. Res. Sci. Eng. Technol.* **2013**, *2*, 687–690.
68. Azhdarpour, A.M.; Nikoudel, M.R.; Taheri, M. The effect of using polyethylene terephthalate particles on physical and strength-related properties of concrete; a laboratory evaluation. *Constr. Build. Mater.* **2016**, *109*, 55–62. [[CrossRef](#)]
69. Lakshmi, R.; Nagan, S. Investigations on Durability Characteristics of E-Plastic Waste Incorporated Concrete. *Asian J. Civ. Eng. (Build. Hous.)* **2011**, *12*, 773–787.
70. Babafemi, A.J.; Šavija, B.; Paul, S.C.; Anggraini, V. Engineering properties of concrete with waste recycled plastic: A review. *Sustainability* **2018**, *10*, 3875. [[CrossRef](#)]
71. Alqahtani, F.K.; Khan, M.I.; Ghataora, G.; Dirar, S. Production of recycled plastic aggregates and its utilization in concrete. *J. Mater. Civ. Eng.* **2017**, *29*, 4016248. [[CrossRef](#)]
72. Manjunatha, M.; Seth, D.; Balaji, K.; Chilukoti, S. Influence of PVC waste powder and silica fume on strength and microstructure properties of concrete: An experimental study. *Case Stud. Constr. Mater.* **2021**, *15*, e00610.
73. Khedr, S.A.; Abou-Zeid, M.N. Characteristics of silica-fume concrete. *J. Mater. Civ. Eng.* **1994**, *6*, 357–375. [[CrossRef](#)]
74. Nochaiya, T.; Wongkeo, W.; Chaipanich, A. Utilization of fly ash with silica fume and properties of Portland cement–fly ash–silica fume concrete. *Fuel* **2010**, *89*, 768–774. [[CrossRef](#)]
75. Islam, M.J.; Meherier, M.S.; Islam, A.K.M.R. Effects of waste PET as coarse aggregate on the fresh and harden properties of concrete. *Constr. Build. Mater.* **2016**, *125*, 946–951. [[CrossRef](#)]
76. Pezzi, L.; De Luca, P.A.; Vuono, D.; Chiappetta, F.; Nastro, A. Concrete products with waste's plastic material (bottle, glass, plate). *Mater. Sci. Forum.* **2006**, *514*, 1753. [[CrossRef](#)]
77. Lee, Z.H.; Paul, S.C.; Kong, S.Y.; Susilawati, S.; Yang, X. Modification of waste aggregate PET for improving the concrete properties. *Adv. Civ. Eng.* **2019**, *2019*, 1–10. [[CrossRef](#)]
78. Haghghatnejad, N.; Mousavi, S.Y.; Khaleghi, S.J.; Tabarsa, A.; Yousefi, S. Properties of recycled PVC aggregate concrete under different curing conditions. *Constr. Build. Mater.* **2016**, *126*, 943–950. [[CrossRef](#)]
79. Liu, F.; Yan, Y.; Li, L.; Lan, C.; Chen, G. Performance of recycled plastic-based concrete. *J. Mater. Civ. Eng.* **2015**, *27*, A4014004. [[CrossRef](#)]
80. Babu, D.S.; Babu, K.G.; Wee, T.H. Properties of lightweight expanded polystyrene aggregate concretes containing fly ash. *Cem. Concr. Res.* **2005**, *35*, 1218–1223. [[CrossRef](#)]
81. British Standard Institution. *Eurocode 2: Design of Concrete Structures-Part 1–1: General Rules and Rules for Buildings*; British Standard Institution: London, UK, 2005.
82. Almehsal, I.; Tayeh, B.A.; Alyousef, R.; Alabduljabbar, H.; Mohamed, A.M. Eco-friendly concrete containing recycled plastic as partial replacement for sand. *J. Mater. Res. Technol.* **2020**, *9*, 4631–4643. [[CrossRef](#)]
83. NZS 3101; Concrete Structures Standard. Standards New Zealand: Wellington, New Zealand, 2006.
84. Neville, A.M.; Brooks, J.J. *Concrete Technology*; Longman Scientific & Technical England: London, UK, 1987.
85. ACI 318-11; Building Code Requirement for Structural Concrete and Commentary. American Concrete Institute: Farming Hills, MI, USA, 2011.

86. Oluokun, F.A.; Burdette, E.G.; Deatherage, J.H. Splitting tensile strength and compressive strength relationships at early ages. *Mater. J.* **1991**, *88*, 115–121.
87. Iranian National Building Codes Compilation Office. *Iranian National Building Code, Part 9: Reinforced Concrete Buildings Design*; Ministry of Housing and Urban Development (MHUD): Washington, DC, USA, 2014.
88. Suzuki, M.; Wilkie, C.A. The thermal degradation of acrylonitrile-butadiene-styrene terpolymer as studied by TGA/FTIR. *Polym. Degrad. Stab.* **1995**, *47*, 217–221. [[CrossRef](#)]
89. Yang, S.; Castilleja, J.R.; Barrera, E.V.; Lozano, K. Thermal analysis of an acrylonitrile-butadiene-styrene/SWNT composite. *Polym. Degrad. Stab.* **2004**, *83*, 383–388. [[CrossRef](#)]
90. Alarcon-Ruiz, L.; Platret, G.; Massieu, E.; Ehrlacher, A. The use of thermal analysis in assessing the effect of temperature on a cement paste. *Cem. Concr. Res.* **2005**, *35*, 609–613. [[CrossRef](#)]
91. Grattan-Bellew, P.E. Microstructural investigation of deteriorated Portland cement concretes. *Constr. Build. Mater.* **1996**, *10*, 3–16. [[CrossRef](#)]

Disclaimer/Publisher's Note: The statements, opinions and data contained in all publications are solely those of the individual author(s) and contributor(s) and not of MDPI and/or the editor(s). MDPI and/or the editor(s) disclaim responsibility for any injury to people or property resulting from any ideas, methods, instructions or products referred to in the content.